MCB
Journals.ASM.org

Human Monocyte Recognition of Adenosine-Based Cyclic Dinucleotides Unveils the A2a $G_{\alpha s}$ Protein-Coupled Receptor Tonic Inhibition of Mitochondrially Induced Cell Death

Marie Tosolini,[a,b,c,d,e] Frédéric Pont,[a,b] Delphine Bétous,[a,b,c,d,e] Emmanuel Ravet,[f] Laetitia Ligat,[a,b] Frédéric Lopez,[a,b] Mary Poupot,[a,b,c,d,e] Marc Poirot,[a,b] Éric Pérouzel,[f] Gérard Tiraby,[f] Els Verhoeyen,[g,h] Jean-Jacques Fournié[a,b,c,d,e]

INSERM UMR1037, Centre Recherches en Cancérologie de Toulouse, Toulouse, France[a]; Université Toulouse III Paul-Sabatier, Toulouse, France[b]; ERL 5294 CNRS, Hôpital Purpan, Toulouse, France[c]; Laboratoire d'Excellence TOUCAN, Toulouse, France[d]; Institut Carnot CALYM, Pierre-Benite, France[e]; Cayla-InVivoGen, Montaudran, France[f]; CIRI, EVIR team, INSERM U1111, CNRS UMR5308, Université de Lyon-1, ENS de Lyon, Lyon, France[g]; INSERM U1065, Centre Méditerranéen de Médecine Moléculaire, Nice, France[h]

Cyclic dinucleotides are important messengers for bacteria and protozoa and are well-characterized immunity alarmins for infected mammalian cells through intracellular binding to STING receptors. We sought to investigate their unknown extracellular effects by adding cyclic dinucleotides to the culture medium of freshly isolated human blood cells *in vitro*. Here we report that adenosine-containing cyclic dinucleotides induce the selective apoptosis of monocytes through a novel apoptotic pathway. We demonstrate that these compounds are inverse agonist ligands of A2a, a $G_{\alpha s}$-coupled adenosine receptor selectively expressed by monocytes. Inhibition of monocyte A2a by these ligands induces apoptosis through a mechanism independent of that of the STING receptors. The blockade of basal (adenosine-free) signaling from A2a inhibits protein kinase A (PKA) activity, thereby recruiting cytosolic p53, which opens the mitochondrial permeability transition pore and impairs mitochondrial respiration, resulting in apoptosis. A2a antagonists and inverse agonist ligands induce apoptosis of human monocytes, while A2a agonists are antiapoptotic. *In vivo*, we used a mock developing human hematopoietic system through NSG mice transplanted with human $CD34^+$ cells. Treatment with cyclic di-AMP selectively depleted A2a-expressing monocytes and their precursors via apoptosis. Thus, monocyte recognition of cyclic dinucleotides unravels a novel proapoptotic pathway: the A2a $G_{\alpha s}$ protein-coupled receptor (GPCR)-driven tonic inhibitory signaling of mitochondrion-induced cell death.

Purine and pyrimidine-based signaling is a fundamental and conserved mode of intercellular communication. In the body, mononucleotides are the major mediators of tissue protection and regeneration, for example, adenosine, which is released from damaged cells. In contrast, microorganisms use cyclic dinucleotides, such as cyclic di-AMP (c-di-AMP) and cyclic di-GMP (c-di-GMP), which are secreted by bacteria and protozoa, respectively (1, 2). As a defense mechanism, mammalian cells have evolved a means to sense cyclic dinucleotides. When infected with retroviruses (3) or carrying cytosolic DNA (4), cells assemble an endogenous 2′,3′ cyclic GMP-AMP (cGAMP) dinucleotide which is recognized by the intracellular protein STING to induce type I interferon (IFN) responses (5). In this way, intracellular cyclic dinucleotides represent important alarmins in immunity.

Extracellular cyclic dinucleotides are released from infected dying cells or damaged tissues and also represent important signals, but whether and how mammalian cells can detect these and respond is presently unknown. We hypothesized that human peripheral blood cells might be capable of detecting extracellular cyclic dinucleotides. We found that the extracellular 3′,5′ cyclic dinucleotides c-di-AMP and cGAMP are specifically recognized by human monocytes expressing the A2a adenosine receptor and can selectively induce their apoptosis. Analysis of the role of A2a in this apoptotic response showed that it controls the survival of the monocytes through its constitutive signaling.

MATERIALS AND METHODS

Reagents. 3′,5′ c-di-AMP, cGAMP, c-di-GMP, c-di-IMP, and c-di-UMP were from InvivoGen. Adenosine, caffeine, 8-cyclopentyl-1,3-dipropylxanthine (DPCPX), forskolin, prostanglandin E2 (PGE2), and cyclosporine were from Sigma-Aldrich (St. Louis, MO). SCH442416, CGS21680, and ZM241385 were from Tocris Biosciences (R&D Systems, Minneapolis, MN). Lactacystin and MG132 were from Interchim (Montlucon, France). Suramin was from Alexis Biochemicals (Lufelfingen, Switzerland). NECA-fluo was from Abcam (Paris, France). Calcein AM, Mitotracker green, and Mitotracker deep red were from Invitrogen (Cergy Pontoise, France). The cXMP and cAMP standards were from the Biolog Life Science Institute (Bremen, Germany). thrombopoietin (TPO), stem cell factor (SCF), and Flt-3 ligand (Flt-3L) were purchased from Preprotech (Neuilly-Sur-Seine, France).

Cell description and isolation procedure. Buffy coats were diluted with phosphate-buffered saline (PBS) in Ficoll separation medium and centrifuged at 400 × *g* for 30 min at 20°C. Human peripheral blood mononuclear cells (PBMCs) obtained in interphase were washed twice with PBS. Then cells were suspended in medium and treated immediately.

Monocytes were purified from freshly isolated human PBMCs using a

Received 30 September 2014 **Returned for modification** 14 October 2014
Accepted 3 November 2014

Accepted manuscript posted online 10 November 2014

Citation Tosolini M, Pont F, Bétous D, Ravet E, Ligat L, Lopez F, Poupot M, Poirot M, Pérouzel E, Tiraby G, Verhoeyen E, Fournié J-J. 2015. Human monocyte recognition of adenosine-based cyclic dinucleotides unveils the A2a $G_{\alpha s}$ protein-coupled receptor tonic inhibition of mitochondrially induced cell death. Mol Cell Biol 35:479–495. doi:10.1128/MCB.01204-14.

Address correspondence to Jean-Jacques Fournié, jean-jacques.fournie@inserm.fr.

doi:10.1128/MCB.01204-14

Dynabeads Untouched human monocyte isolation kit (Invitrogen, Cergy Pontoise, France) (final purity of $CD14^+$ cells = 95%).

To differentiate macrophages from dendritic cells (DC), PBMCs were allowed to adhere to the substratum for 2 h before nonadherent cells were removed by washing the wells three times. Adherent cells were then cultured for 6 days to allow monocytes to differentiate into either type 1 macrophages (M1) using IFN-γ (100 U/ml) and lipopolysaccharide (LPS; 10 ng/ml), type 2 macrophages (M2) using interleukin 4 (IL-4; 300 U/ml), or immature dendritic cells (iDC) using IL-4 (150 U/ml) and granulocyte-macrophage colony-stimulating factor (GM-CSF; 10 ng/ml). To induce dendritic cell maturation, LPS (20 ng/ml) was added to the iDC culture for the final 2 days of culture. M1, M2, iDC, and mature DC phenotypes were analyzed by flow cytometry using antibodies against CD80, CD86, CD83, HLA-DR, HLA ABC, CD1a, and CD64.

C57BL/6 mice were sacrificed in accordance with bioethical procedures. The spleen, thymus, peripheral blood, and bone marrow were harvested. Cells from the spleen and thymus were separated by crushing them through a mesh (40 μm). Blood was taken from the retro-orbital vein and bone morrow was obtained by flushing the femurs of the mice with PBS using a 29-gauge needle. The mononuclear cell fraction was obtained by centrifugation in a Ficoll density gradient.

Cell assays. Freshly isolated peripheral blood mononuclear cells or purified monocytes from healthy donors were cultured at 37°C and 5% CO_2 at 1.5×10^6 cells/ml in RPMI medium supplemented with 10% heat-inactivated fetal calf serum (FCS), 2 mM L-glutamine, 100 U/ml of penicillin, and 100 μg/ml of streptomycin (Invitrogen). Splenocytes isolated from C57BL/6 mice were cultured in the same medium supplemented with 20 mM HEPES. The desired 3′,5′ cyclic dinucleotides were added to the cultures at 5 μM unless specified otherwise. After 16 h, cells were stained with the appropriate monoclonal antibodies or reagents and analyzed by flow cytometry. The same settings were used for competition assays with A2a ligands, although these ligands were added 1 h prior to c-di-AMP addition. The $A2a^+$ human monocyte line THP1-Blue-ISG-hSEAP (InvivoGen, Montaudran, France) was cultured as described above. Upon activation of human STING, the THP1-Blue-ISG-hSEAP monocyte cell line secretes an embryonic alkaline phosphatase (hSEAP) reporter gene under the control of an ISG54 promoter in conjunction with five IFN-stimulated response elements. The hSEAP secreted in the cell culture supernatant is revealed by a colorimetric reaction according to the supplier's instructions. The Chinese hamster ovary (CHO) cell line was cultured in Ham's F-12 medium containing 10% fetal bovine serum (FBS) and was transfected with an A2a receptor construct (in pcDNA3) using LyoVec (InvivoGen) according to the manufacturer's instructions. Twenty-four hours after transfection, CHO cells were treated with CGS21680 (100 nM) or c-di-AMP (10 μM) for 5 min before phosphorylated extracellular signal-regulated kinase 1/2 (phospho-ERK1/2) staining.

Flow cytometry. Monoclonal antibodies used for the staining of cells were phycoerythrin (PE)-Cy7 conjugated anti-CD14; PE active caspase 3 apoptosis kit, phospho-ERK1/2, ERK2, and p53 set (p53 fluorescein isothiocyanate [FITC], clone G59-12, and isotype control, clone MOPC-21) (BD Biosciences, Pont de Claix, France); phospho-p53 (Ser315) antibody (Antibodies-Online GmbH, Aachen, Germany); and BV421-conjugated anti-CD3 (BioLegend, Ozyme, Saint-Quentin-en-Yvelines, France). Mitochondrial function was assessed using Mitotracker deep red and Mitotracker green (both at 25 nM) as described in reference 6. Cell viability was measured with 7-amino-actinomycin D (7-AAD) and annexin V (BD Biosciences) staining according to the manufacturer's instructions. Briefly, PBMCs or purified cells were washed twice with ice-cold PBS containing 1% FCS, stained on ice for 30 min with the specified antibodies, then washed, and analyzed using a BD LSR II cytometer (BD Biosciences, Pont de Claix, France). Data were processed with Cytobank software (http://www.cytobank.org) and are represented as contour plots.

Monocyte morphology. Purified monocytes were treated with 125 ng/ml of anti-FAS (2R2; eBiosciences, Paris, France), 10% ethanol, or 0.6 μM c-di-AMP for 7 h. Cells were then stained for 15 min at 37°C with 100 μg/ml of acridine orange (AO) and 1 μg/ml of 4′,6-diamidino-2-phenylindole (DAPI; Life Technologies, Saint Aubin, France) prior to being washed. Cells were then stained with annexin V-PE (BD Biosciences, Le Pont de Claix, France), then washed, and photographed with a Nikon Eclipse TE200 fluorescence microscope (magnification, ×40).

TABLE 1 Probe sets used for human and mouse adenosine receptor-encoding genes

Gene	Human probe	Murine probe
Adora1	216220_s_at	1427331_at
Adora2a	205013_s_at	1460710_at
Adora2b	205891_at	1450214_at
Adora3	206171_at	1429609_at
P2rx1	210401_at	1460719_a_at
P2rx2	221356_x_at	1435212_at
P2rx3	208338_at	1458396_at
P2rx4	204088_at	1425525_a_at
P2rx5	210448_s_at	1449433_at
P2rx6	206880_at	1450327_at
P2rx7	207091_at	1439787_at
P2ry1	207455_at	1421456_at
P2ry2	206277_at	1450318_a_at
P2ry4	221466_at	1422276_at
P2ry5	218589_at	
P2ry6	208373_s_at	1425214_at
P2ry8	229686_at	
P2ry10	1553856_s_at	1452815_at
P2ry11	214546_s_at	
P2ry12	235885_at	1431724_a_at
P2ry13	220005_at	1428700_at
P2ry14	206637_at	1424733_at
Gapdh	humgapdh-M33197_3_at	GapdhMur-M32599

Microarray data mining. Transcriptomes from human PBMCs obtained with the Affymetrix Human Genome U133 Plus 2.0 platform were produced in our laboratory (monocytes, γδ T cells, and NK cells) and deposited at the NCBI repository Gene Expression Omnibus (GEO) database (accession numbers GSE42733 and GSE27291) (7). In addition, the B cell and γδ T cell transcriptomes were downloaded from the NCBI repository GEO database (accession numbers GSE12195 and GSE15659, respectively) (8, 9) prior to normalization in batch by the RMA software. Myeloid and $CD34^+$ human cell transcriptomes were from the NCBI repository GEO database (accession number GSE19599) (10). Transcriptomes from murine splenocytes obtained with the Affymetrix Mouse Genome 430 2.0 array were downloaded from the NCBI repository GEO data sets under accession numbers GSE22196 (γδ T cells) and GSE27787 (other subsets) prior to normalization in batch by RMA. The probe sets used for human and mouse adenosine receptor-encoding genes are listed in Table 1.

All data are expressed as arbitrary units relative to the expression of glyceraldehyde-3-phosphate dehydrogenase (GAPDH).

SPR assays. All binding studies based on surface plasmon resonance (SPR) technology were performed on a BIAcore T200 optical biosensor instrument (GE Healthcare). The immobilization of biotinylated c-di-AMP was performed on a streptavidin-coated (SA) sensor chip in HBS-EP buffer (10 mM HEPES [pH 7.4], 150 mM NaCl, 3 mM EDTA, 0.005% surfactant P20) (GE Healthcare). All immobilization steps were performed at a flow rate of 2 μl/min with a final c-di-AMP concentration of 100 μg/ml. The total amount of immobilized c-di-AMP was 250 resonance units (RU). CHO cells were lysed in 20 mM HEPES–10 mM EDTA (pH 7.4) by freeze-thaw cycles. Binding analyses were performed with solubilized purified mock-transfected CHO (FC1) and CHO-A2a (FC2) cell membrane proteins at 11 μg/μl over the immobilized c-di-AMP sur-

face at 25°C for 3 min at a flow rate of 30 μl/min. The channel (Fc1) was used as a reference surface for nonspecific binding measurements. Immobilization of membrane extract proteins was performed on an L1 sensor chip in HBS-N buffer (10 mM HEPES [pH 7.4], 150 mM NaCl) (GE Healthcare). All immobilization steps were performed at a flow rate of 2 μl/min with final concentrations of mock-transfected CHO and CHO-A2a cells of 6 μg/μl. The total amount of immobilized membrane protein was about 400 RU each. A channel (Fc2) was used for the immobilization of CHO-A2a cell proteins, and a channel with immobilized mock-transfected CHO cell proteins (Fc1) was used as a reference surface for nonspecific binding measurements. Binding analyses were performed with c-di-AMP at 100 μM over the immobilized mock-transfected CHO and CHO-A2a cell surface at 25°C for 3 min at a flow rate of 30 μl/min.

Molecular modeling and dockings. The crystallized conformation of A2a-bound agonists and antagonists were obtained from UK432097 (an analog of CGS21680; Protein Data Bank [PDB] code 3QAK), adenosine (5-*N*-ethyl-carboxamido-adenosine [NECA]; PDB code 2YDV), caffeine (PDB code 3RFM), xanthine amine congener (XAC) (PDB code 3REY), and ZM241385 (an allosteric inverse agonist of A2a; PDB code 3PWH), while the corresponding conformation of istradefylline was based upon published reports (11, 12). These ligands were aligned using their respective Asn253-binding atoms as a reference. The docking experiments were performed with SwissDock (http://swissdock.vital-it.ch/) (13), using the CHARMM force field, MOL2 or PDB files of ligands, and the crystal structure of the active (PDB code 2YDV) and inactive (PDB code 3PWH) A2a. The binding site was defined by a 10-Å sphere around the cocrystallized ligand. The cocrystallized ligand and detergent were then removed from the crystal structure, while all waters were retained before docking. Dockings were done in the accurate mode restricted to a 10-Å sphere around the putative binding pocket, applying flexibility for side chains within 5 Å of any atom of the ligand in its reference binding mode. Up to 250 poses per ligand were stored, scored, and clustered according to the average full fitness of their elements. All poses were ranked according to their estimated ΔG (kcal/mol), loaded as PDB files, and visually inspected using the ViewDock plugin of the molecular viewer UCSF Chimera (version 1.7, build 38197; Resource for Biocomputing Visualization and Informatics at the University of California, San Francisco, CA) to identify the best docking. Figures were generated using UCSF Chimera and PyMOL (The PyMOL molecular graphics system, version 1.5x; Schrödinger, LLC).

siRNA transfection. Freshly isolated human PBMCs were transfected with A2a or control small interfering RNA (siRNA) using an siRNA reagent system (Santa Cruz Biotechnology) according to the manufacturer's instructions and cultured with gentle shaking (180 rpm).

Measurement of intracellular cAMP. Because the intracellular level of the cAMP second messenger could not be measured by antibody-based assays due to cross-reactivity with c-di-AMP or cGAMP (G. Lebon, personal communication), this dosage was performed by liquid chromatography-mass spectrometry (LC-MS) (14), with modifications for MS_n selected multi-ion analysis. Briefly, purified monocytes (95% $CD14^+$ cells) were cultured (5 million/well) with or without c-di-AMP (5 μM) for 16 h in complete medium supplemented with 3-isobutyl-1-methylxanthine (IBMX) (45 μM) and then collected, washed, and extracted with acetonitrile-methanol-water (40:40:20, vol/vol/vol). Each sample was then spiked with 40 pmol of a quantification standard of 3′,5′ cyclic xanthine monophosphate (cXMP). Extracts were left for 15 min at 4°C, heat inactivated (10 min at 95°C), and then pelleted by centrifugation, and supernatants were collected and concentrated using a rotating speed vacuum (100 × *g* at room temperature for 2 h) and adjusted to a final volume of 50 μl for LC-MS. Samples (50 μl) were injected and separated on a 50- by 2-mm Prontosil C_{18} column (3 μm, 120-Å porosity; Bischoff, Leonberg, Germany) using a sequential elution program involving solvent A (0.1% formic acid) and solvent B (acetonitrile). The elution program was 10 min of 100% solvent A, 3 min at a gradient of 0 to 100% solvent B, and then 2 min of 100% solvent B. The flow rate was 250 μl/min. For detection, a UV6000 LP photodiode array (SpectraSYSTEM; Thermo Scientific, France) was used over a λ of 200 to 500 nm, with faster acquisition at a λ of 254 nm, followed by electrospray ion trap mass spectrometry (Finnigan-LCQ, USA). Detection in the negative mode involved full-scan MS/MS (range, 90 to 400 amu) with the two precursor ions of *m/z* 328 for cAMP and *m/z* 345 for the cXMP standard. Diagnostic ions for integration were at *m/z* 134 for cAMP (collision energy, 34%) and *m/z* 151 for cXMP (collision energy, 30%). The daughter ion at *m/z* 247 was also used for validation of cXMP, while the fragmentation pattern of cAMP in the negative mode gave only the fragment at *m/z* 134. The baseline amount of intracellular cAMP in control human monocytes was 59 ± 10 pmol of cAMP per million cells.

PKA activity. Purified monocytes (0.3 million/well) cultured with or without c-di-AMP (5 μM) in complete medium were collected at the desired time points, washed, and extracted. Protein kinase A (PKA) activities were measured using the PKA activity kit (Enzo Life Sciences, Villeurbanne, France) according to the manufacturer's instructions. Briefly, precoated substrate was incubated with the extracted protein (2 μg per point) and ATP and was revealed with a phospho-specific substrate antibody.

Western blotting and cell fractionation. Purified monocytes (final purity of $CD14^+$ cells = 95%) were cultured for 16 h with or without c-di-AMP (5 μM). Cells were lysed using buffer composed of 10 mM HEPES (pH 7.9), 10 mM KCl, 1.5 mM $MgCl_2$, 0.34 mM sucrose, 10% glycerol, 1 mM dithiothreitol (DTT), 0.1% Triton X-100, 5 μg/ml of aprotinin, 5 μg/ml of leupeptin, 0.5 μg/ml of pepstatin, and 0.1 mM phenylmethylsulfonyl fluoride (PMSF) for 5 min on ice, followed by centrifugation (1,300 × *g*, 4 min, and 4°C). The supernatants, composed of the cytoplasmic fraction, were centrifuged at 20,000 × *g* and 4°C for 15 min to remove insoluble proteins. The pellets containing the nuclei were washed using the same buffer and lysed with 3 mM EDTA, 0.2 mM EGTA, and 1 mM DTT for 30 min on ice, followed by sonication for 15 s. Samples were quantified by the bicinchoninic acid (BCA) protein assay (Sigma-Aldrich), and the same amounts of proteins per lane were analyzed. Antibodies were for α-tubulin (Sigma-Aldrich), β-actin (Millipore, Molsheim, France), Orc2 (Clinisciences, Montrouge, France), and total p53 (DO-1 clone; Santa Cruz Biotechnology) and peroxidase-conjugated anti-rabbit or anti-mouse Ig (Jackson ImmunoResearch Laboratories, Montluon, France).

mPTP flow cytometry assay. The mitochondrial permeability transition pore (mPTP) was measured as described previously (15), with modifications for flow cytometry. Briefly, PBMCs were treated as specified below with cyclosporine (10 μM), CGS21680 (100 μM), forskolin (100 μM), or c-di-AMP (5 μM) for 6 h and then loaded with membrane-permeant acetoxymethyl-calcein ester (100 nM) and the cytosolic calcein fluorescence quencher $CoCl_2$ (0.4 mM) for 15 min at 37°C. At the same time, mitochondrial function was assessed using Mitotracker deep red staining (25 nM for 30 min at 37°C). In control experiments, cells were loaded with acetoxymethyl-calcein alone. Cells were centrifuged, washed, stained with antibodies, and analyzed by flow cytometry. The mPTP was measured by mitochondrial calcein and Mitotracker red signals on gated monocytes ($CD14^+$ $CD3^-$ cells).

Bioenergetic profiling. Purified monocytes (final purity of $CD14^+$ cells = 95%) were resuspended in XF base medium (supplemented with 2 mM L-glutamine, 1 mM pyruvate, and 10 mM glucose [pH 7.4]) and plated (250,000 cells/well) in 96-well CellTak (Corning)-coated assay plates. Cellular bioenergetics were determined using an extracellular flux analyzer (Seahorse; Proteigen, France) according to the manufacturer's instructions. Briefly, cells were incubated in the analyzer, with measurements of the O_2 consumption rate (OCR) and the extracellular acidification rate (ECAR) taken every 5 min. Treatments (5 μM c-di-AMP) were added after 3 cycles of measurement, and evolution of the baseline was followed for 6 h. At the end of the experiment, drugs for inhibiting mitochondrial function were injected to determine the capacity of mitochondrial function. Protein quantity was used to reflect the quantity of cells in each well and to normalize the results.

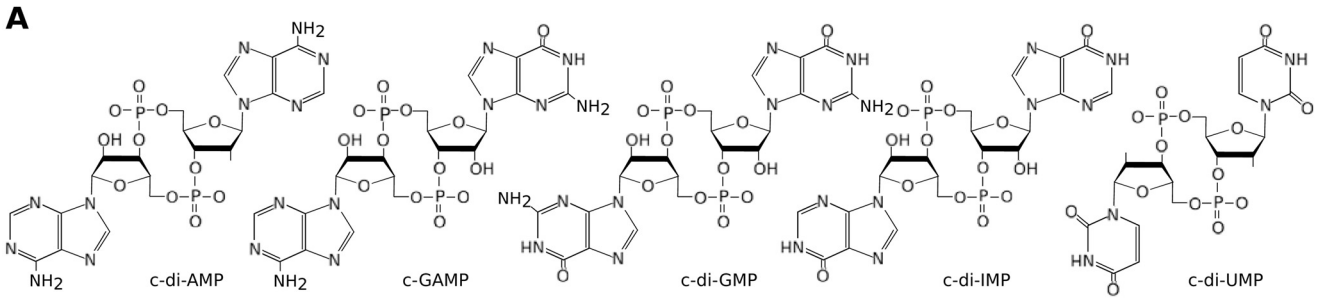
A
c-di-AMP
c-GAMP
c-di-GMP
c-di-IMP
c-di-UMP

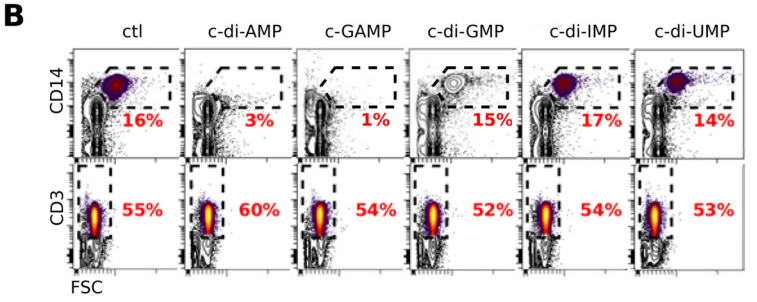
B
ctl
c-di-AMP
c-GAMP
c-di-GMP
c-di-IMP
c-di-UMP
CD14
CD3
16%
3%
1%
15%
17%
14%
55%
60%
54%
52%
54%
53%
FSC

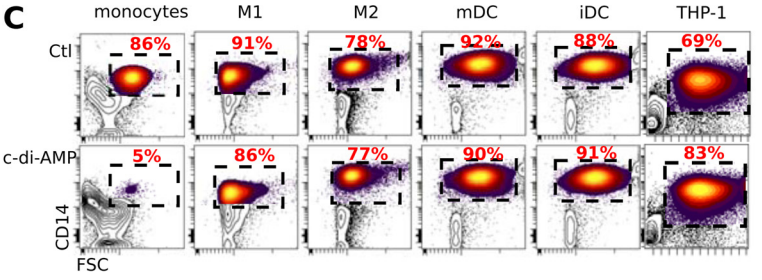
C
monocytes
M1
M2
mDC
iDC
THP-1
Ctl
c-di-AMP
CD14
86%
91%
78%
92%
88%
69%
5%
86%
77%
90%
91%
83%
FSC

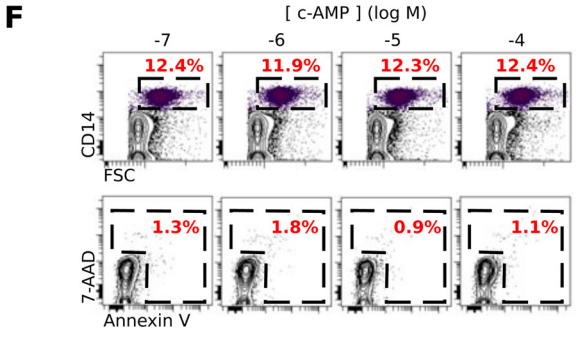
F
[c-AMP] (log M)
-7
-6
-5
-4
CD14
12.4%
11.9%
12.3%
12.4%
FSC
7-AAD
1.3%
1.8%
0.9%
1.1%
Annexin V

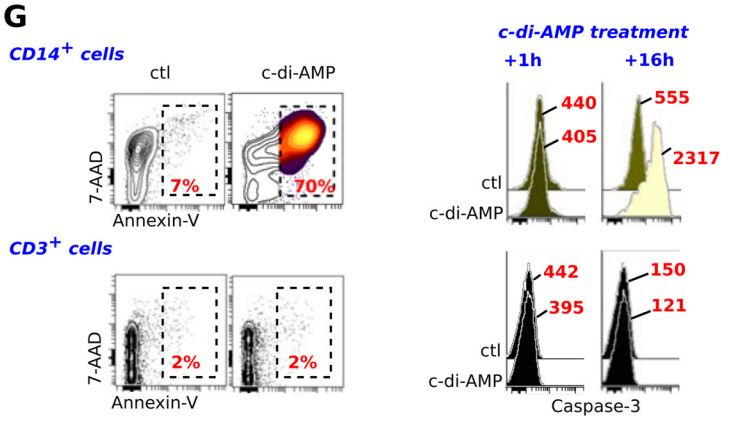
G
CD14+ cells
ctl
c-di-AMP
7-AAD
7%
70%
Annexin-V
CD3+ cells
2%
2%
c-di-AMP treatment
+1h
+16h
440
405
555
2317
ctl
c-di-AMP
442
395
150
121
Caspase-3

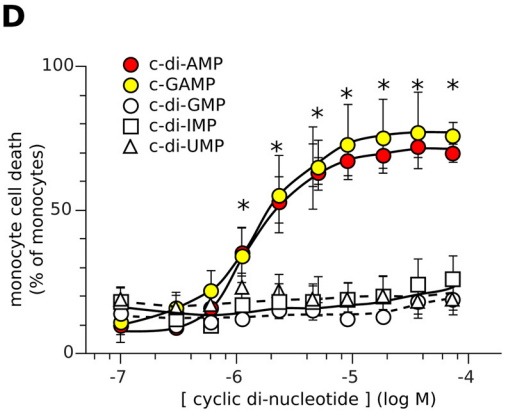
D
c-di-AMP
c-GAMP
c-di-GMP
c-di-IMP
c-di-UMP
monocyte cell death
(% of monocytes)
[cyclic di-nucleotide] (log M)

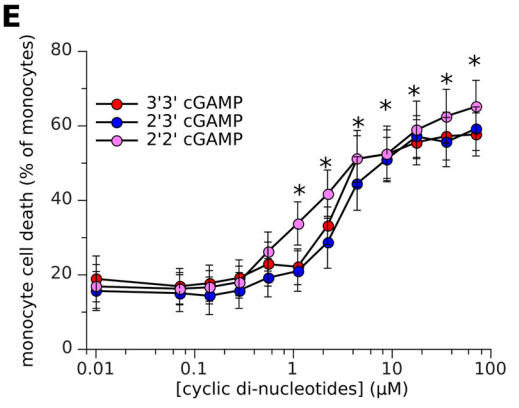
E
3'3' cGAMP
2'3' cGAMP
2'2' cGAMP
monocyte cell death (% of monocytes)
[cyclic di-nucleotides] (μM)

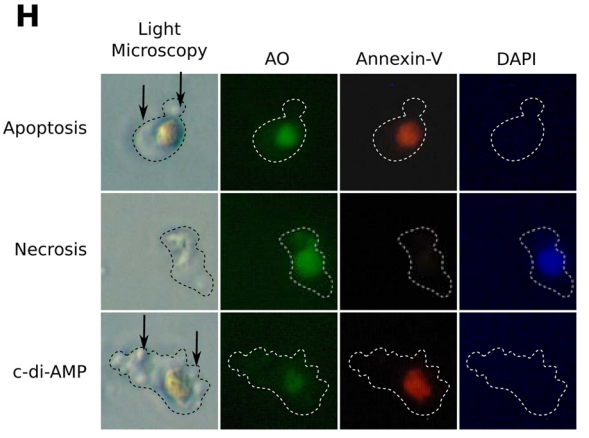
H
Light
Microscopy
AO
Annexin-V
DAPI
Apoptosis
Necrosis
c-di-AMP

NSG mice reconstituted with human hematopoietic cells. Cord blood (CB) samples were collected in sterile tubes containing the anticoagulant acid citrate dextrose (ACD; Sigma, France) after informed consent by Etablissement Français du Sang (EFS; Lyon, France) according to the Helsinki declaration. Purified $CD34^+$ cells from cord blood were stimulated for 16 to 18 h with a cytokine cocktail (TPO, 20 ng/ml; SCF, 100 ng/ml; and Flt-3L, 100 ng/ml). NOD/SCID/$\gamma_c^{-/-}$ (NSG) mice were housed in a dedicated animal facility (PBES, Lyon, France), and experiments were performed according to the guidelines of the institutional animal care committee with approval by the local ethics committee. Two- to 3-day-old newborn NSG mice were subjected to irradiation at 1 Gy, and 2×10^5 cytokine-prestimulated (TPO, 20 ng/ml; SCF, 100 ng/ml; and Flt-3L, 100 ng/ml) human cord blood $CD34^+$ cells were injected intrahepatically. Upon 8 weeks of reconstitution, the percentage of human $CD45^+$ cells in the blood was determined every week to follow human cell engraftment. Mice with >30% human $CD45^+$ cells were injected intravenously with 100 μl of PBS or c-di-AMP (50 μg). This procedure was repeated after 48 h, and the mice were sacrificed 48 h after the last c-di-AMP injection. The different hematopoietic tissues (bone marrow, spleen, thymus, and blood) of these primary mice were stained for CD45-allophycocyanin (CD45-APC) and CD14-APC-Cy7 combined with annexin-PE–7-AAD to detect apoptotic cells. Additionally, the marking of human B cells (CD19-APC), T cells (CD3-PE-Cy7), and myelocytes (CD13-APC) was performed. Fluorescence-activated cell sorter (FACS) analysis was performed using a Canto II (Becton Dickinson).

Statistical analysis. Data are expressed as means ± standard deviations (SD), as specified below. Differences between groups versus the specified controls were analyzed using the paired two-tailed Student *t* test.

RESULTS

Adenosine-based cyclic dinucleotides induce the selective apoptosis of human monocytes. We added various 3′,5′ cyclic dinucleotides, namely, c-di-AMP, cGAMP, c-di-GMP, c-di-UMP, and c-di-IMP (Fig. 1A), to short-term *in vitro* cultures of freshly isolated human peripheral blood mononuclear cells (PBMCs). Within 16 h a selective loss of $CD14^+$ monocytes was observed with c-di-AMP and cGAMP, whereas $CD3^+$ and the other PBMC subsets were completely unaffected (Fig. 1B). In contrast, differentiated human M1 and M2 macrophages, monocyte-derived DC, and THP1 myeloid cancer cells (Fig. 1C) were not killed by these nucleotides *in vitro*. Moreover, the monocyte-restricted cytotoxicity of these extracellular compounds was specific to the adenosine-containing cyclic dinucleotides (50% inhibitory concentration [IC_{50}], ~1 μM for c-di-AMP and cGAMP) (Fig. 1D). Accordingly, the 2′,3′ cGAMP, 2′,2′ cGAMP, and 3′,3′ cGAMP isomers were as cytotoxic as 3′,5′ cGAMP (Fig. 1E), whereas the closely related cyclic 3′,5′ cAMP mononucleotide was inactive (Fig. 1F). Sixteen hours after c-di-AMP treatment of PBMCs, flow cytometry analysis and visual examination evidenced a monocyte phenotype (7-AAD^+, annexin V^+, and caspase 3^+) (Fig. 1G) with an apoptotic cell morphology similar to that seen with monocytes treated with anti-Fas (annexin V^+, $DAPI^-$ cells) but different from that of necrotic monocytes (annexin V^-, $DAPI^+$) (Fig. 1H). In agreement with these results, the caspase inhibitor zVAD prevented the death of c-di-AMP-treated or c-GAMP-treated monocytes (data not shown). Thus, extracellular cyclic dinucleotides containing adenosine are selectively proapoptotic toward freshly isolated human monocytes.

Human monocytes selectively express Adora2a encoding the A2a adenosine receptor. Cytoplasmic cGAMP and c-di-AMP can bind to the intracellular stimulator of interferon genes (STING) receptor, leading to IFN-β production (5) and cell death by pyroptosis (16). Both cGAMP and c-di-AMP showed a reduced cytotoxicity when transfected into purified monocytes compared to when they were added to the culture medium (Fig. 2A). cGAMP has a higher affinity for intracellular STING than c-di-AMP (3) but shows lower intracellular cytotoxicity than extracellular cytotoxicity, whereas c-di-AMP is equally cytotoxic in both cases. This suggests that the intracellular interaction of cGAMP with STING decreases the extracellular pool of nucleotides, which causes cytotoxicity. Accordingly, the addition of c-di-AMP and cGAMP to the culture medium induced an average release of 124 pg/ml of IFN-β, compared to 8 pg/ml for the control medium (Fig. 2B), while the direct treatment of monocytes with IFN-β (up to 2,000 pg/ml) did not induce their apoptosis (Fig. 2C). These results suggest that STING-induced interferon responses were not responsible for the strong cytotoxicity of the extracellular cyclic dinucleotides. Hence, we postulated that an adenosine receptor located at the cell surface could be present to mediate this potent and selective proapoptotic activity of c-di-AMP and cGAMP. Mining the transcriptomes of human PBMCs for adenosine receptor-encoding genes with a monocyte-selective expression pattern identified only two candidates, Adora2a and P2rx4 (Fig. 2D). The P2rx4 gene was discarded because it encodes a suramin-resistant, ATP-gated cation channel and we had found suramin to be as active as the cyclic dinucleotides (see below). In contrast, Adora2a encodes the adenosine receptor A2a, a $G_{\alpha s}$ protein-coupled receptor (GPCR) that mediates cytoprotection upon binding extracellular adenosine (17). To test for the presence of the receptor at the cell surface, human PBMCs or splenocytes isolated from C57BL/6 mice were labeled with a fluorescent derivative of 5-*N*-ethyl-carboxamido-adenosine (NECA), a potent agonist of A2a (K_i = 20 nM). Their analysis by flow cytometry demonstrated that human but not murine monocytes express A2a at their surface (Fig. 2E). As expected, and in contrast to human monocytes, murine monocytes were not killed by c-di-AMP (Fig. 2F). However, neither classical A2a ligands nor c-di-AMP or cGAMP displaced fluorescent NECA labeling from human monocytes in competition binding assays (data not shown), suggesting that the NECA/A2a

FIG 1 Adenosine-based 3′,5′-cyclic dinucleotides induce the selective apoptosis of human monocytes. (A) Structure of the cyclic dinucleotides. (B) Freshly isolated PBMCs were cultured for 16 h in complete medium with the 3′,5′ cyclic dinucleotides (5 μM) and then stained for CD14 or CD3. ctl, control. (C) Same as for panel B but using monocytes, M1 and M2 macrophages, mature and immature dendritic cells (mDC and iDC, respectively) and the THP1 monocytic cancer cell line. (D) Titration of 3′,5′ cyclic dinucleotide bioactivity on $CD14^+$ monocyte death. Means and SD from 14 independent experiments are shown. *, $P < 0.05$ (Student *t* test) versus untreated control. (E) Titration of 3′,3′, 2′,3′, and 2′,2′ cGAMP bioactivity on $CD14^+$ monocyte death. Shown are means and SD from six independent experiments. *, $P < 0.05$ (paired Student *t* test) versus control. (F) Same as for panel D but using freshly isolated monocytes incubated with cAMP. (G) PBMCs were cultured for 16 h with c-di-AMP (5 μM) and then stained for CD14, CD3, and caspase 3 and labeled with 7-AAD and annexin V prior to flow cytometry analysis of either $CD14^+$ (monocytes) or $CD3^+$ (T lymphocytes) cells. Mean values of caspase 3 fluorescence intensity are indicated. (H) Representative images of monocytes stained with acridine orange (AO), annexin V, and DAPI while dying of apoptosis (anti-FAS treatment for 7 h), necrosis (7 h in 10% ethanol), or c-di-AMP (0.6 μM for 7 h). Arrows indicate membrane blebbing and apoptotic bodies. These data indicate that c-di-AMP induces the selective apoptosis of monocytes.

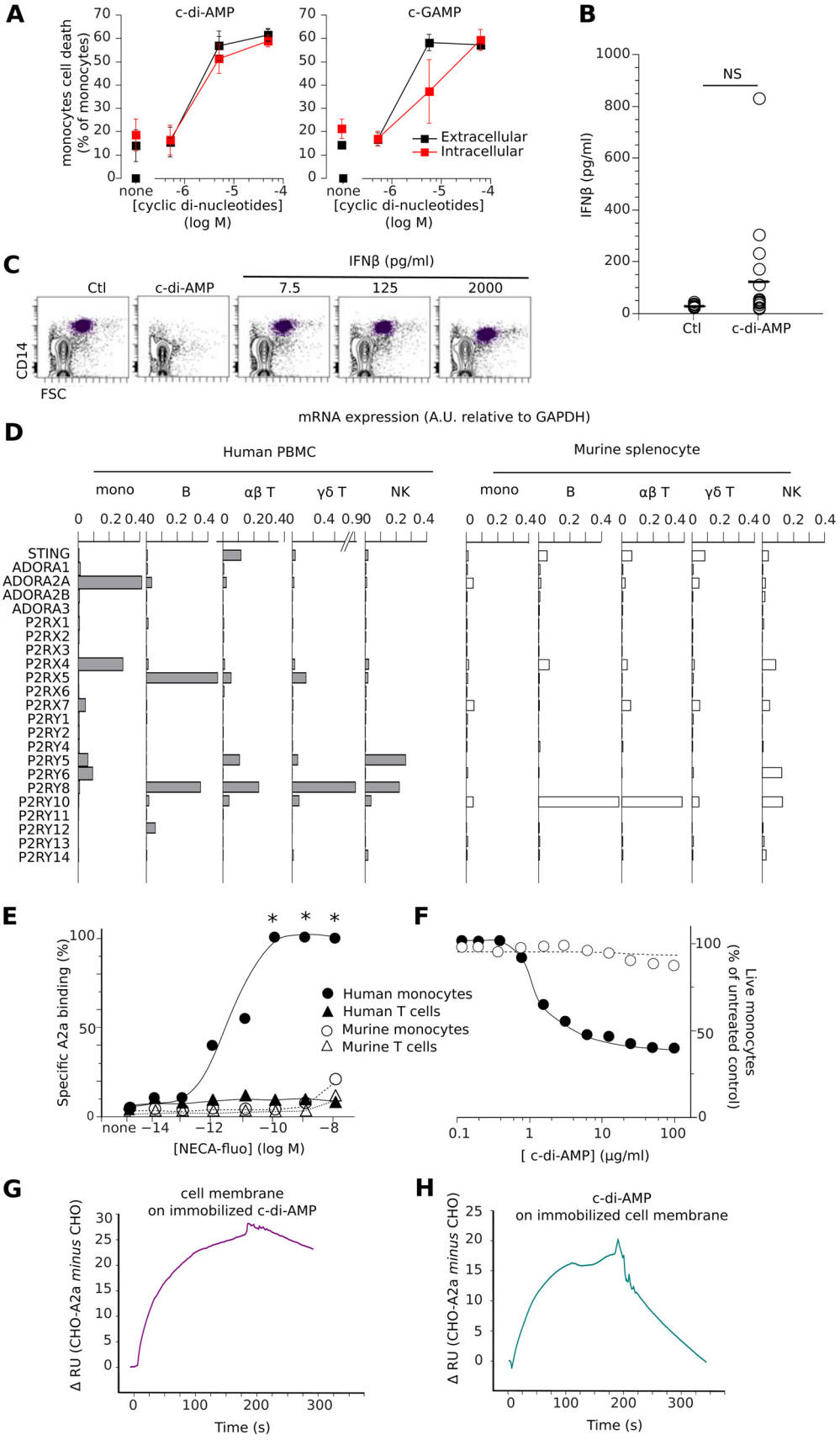
A
c-di-AMP
c-GAMP
monocytes cell death (% of monocytes)
[cyclic di-nucleotides] (log M)
Extracellular
Intracellular
B
IFNβ (pg/ml)
NS
Ctl
c-di-AMP
C
IFNβ (pg/ml)
Ctl
c-di-AMP
7.5
125
2000
CD14
FSC
D
mRNA expression (A.U. relative to GAPDH)
Human PBMC
Murine splenocyte
mono
B
αβ T
γδ T
NK
STING
ADORA1
ADORA2A
ADORA2B
ADORA3
P2RX1
P2RX2
P2RX3
P2RX4
P2RX5
P2RX6
P2RX7
P2RY1
P2RY2
P2RY4
P2RY5
P2RY6
P2RY8
P2RY10
P2RY11
P2RY12
P2RY13
P2RY14
E
Specific A2a binding (%)
[NECA-fluo] (log M)
Human monocytes
Human T cells
Murine monocytes
Murine T cells
F
Live monocytes (% of untreated control)
[c-di-AMP] (µg/ml)
G
cell membrane on immobilized c-di-AMP
Δ RU (CHO-A2a minus CHO)
Time (s)
H
c-di-AMP on immobilized cell membrane
Δ RU (CHO-A2a minus CHO)
Time (s)

complexes had been internalized (18). The sensitivity to adenosine-based cyclic dinucleotides correlated with the expression of the A2a GPCR. Specific c-di-AMP binding to A2a was evaluated using cell membranes purified from the human A2a-transfected Chinese hamster ovary (CHO) cell line, which lacks the A2a receptor. CHO cells were transfected with human A2a, and c-di-AMP binding to A2a was analyzed by comparative Biacore experiments. By comparing the differential of c-di-AMP binding to the cell membrane between A2a-transfected CHO versus mock-transfected CHO cells, we demonstrated that c-di-AMP specifically binds to the A2a receptor (Fig. 2G and H).

c-di-AMP and cGAMP are inverse agonist ligands of the adenosine receptor A2a. The A2a GPCR has inactive and active conformations that are stabilized by antagonist/inverse agonists and agonist ligands, respectively. Stimulation of the active conformation triggers $G_{\alpha s}$ activation of adenylate cyclase to produce cAMP, which then propagates downstream signaling (17). Although we found that c-di-AMP binds A2a, such cyclic dinucleotide ligands could correspond to either agonists or antagonist/inverse agonists. At around 494 $Å^3$, c-di-AMP and cGAMP are larger molecules than most of the known agonist and antagonist ligands of A2a (around 200 $Å^3$). The ligand-binding cavity of A2a measures 200 $Å^3$ in the active state and 518 $Å^3$ in the inactive state, suggesting that these cyclic dinucleotides could only fit in the inactive A2a conformation. Molecular docking methods were used to analyze c-di-AMP and various A2a agonist or antagonist ligands in the cavities of three distinct crystal structures of A2a (PDB codes 2YDV, 3PWH, and 3QAK) (11). These indicated that one c-di-AMP (6′ NH_2) group can interact with the A2a N253 residue without binding to the A2a S277 and H278 residues (Fig. 3A). This interaction pattern can stabilize inactive A2a but not active A2a, as reported for its antagonist ligands (19, 20). Furthermore, a comparison of the putative docking modes of c-di-AMP into the active-state (PDB codes 2YDV and 3QAK) and inactive-state (PDB code 3PWH) crystal structures of A2a indicated a clear thermodynamic preference for binding to the inactive conformation (−7.0 kcal/mol) rather than the active one (−5.0 kcal/mol). This was also seen for the A2a antagonists caffeine and SCH442416 and for the inverse agonists istradefylline and ZM241385 (Fig. 3A) (11). Of all the predicted binding modes for c-di-AMP and cGAMP, the most stable consists of one adenosine lying in the reference ligand-binding site of A2a, while the other moiety (adenosine for c-di-AMP or guanosine for cGAMP) plugs the groove on the top surface of A2a (Fig. 3B and C). These data suggest that dinucleotides bind to the inactive conformation and that they are likely to be antagonists/inverse agonists. In CHO cells transfected with A2a, A2a agonists induce ERK1/2 phosphorylation (21). We thus used ERK1/2 phosphorylation status as confirmation that cyclic dinucleotides are not agonist ligands of A2a. In mock-transfected CHO cells, baseline levels of ERK1/2 were unaffected by the A2a agonist CGS21680 or by c-di-AMP. In contrast, CGS21680 induced ERK1/2 phosphorylation in CHO-A2a cells as previously reported (21), but c-di-AMP did not, confirming that c-di-AMP is not an agonist of A2a. Importantly, CGS21680-induced ERK1/2 phosphorylation in CHO-A2a cells was abrogated by the addition of c-di-AMP to CGS21680, while control CHO cells remained unaffected (Fig. 3D). These results demonstrate that c-di-AMP is an antagonist/inverse agonist ligand of A2a.

Ligands of A2a regulate monocyte apoptosis induced by c-di-AMP and cGAMP. The above data support the notion that c-di-AMP and cGAMP are antagonist/inverse agonist ligands of A2a and suggest this as an A2a-based mechanism for the cyclic dinucleotide-induced apoptosis of human monocytes. If correct, this hypothesis implies that other A2a antagonists/inverse agonists may also be selectively cytotoxic to human monocytes.

To validate this idea, we thus tested A2a agonists and antagonists/inverse agonists using the monocyte apoptosis assay described for Fig. 1. The A2a antagonists caffeine and SCH442416, and the inverse agonist ZM241385, behaved like c-di-AMP (although less efficiently) in selectively depleting monocytes from human PBMCs, while the A2a agonists did not (Fig. 4A). In line with an inverse agonist activity for c-di-AMP, the A2a agonist CGS21680 protected monocytes from the lethality of cyclic dinucleotides (Fig. 4B). Other A2a agonists were also protective, with efficacies related to their 50% effective concentrations (EC_{50}) for this receptor (Fig. 4C to G).

To determine whether the cyclic dinucleotides are antagonists or inverse agonists of A2a, the viabilities of monocytes treated with c-di-AMP in the presence and absence of A2a agonists were compared. We found that the IC_{50} of c-di-AMP was the same (2.5 μM) when added alongside the weak agonist adenosine, when added alongside the potent agonist CGS21680, or in the absence of any A2a agonist (Fig. 4D). Both antagonists and inverse agonists inhibit agonist-induced signaling downstream of GPCRs, but only inverse agonists inhibit their basal agonist-free signaling (22). Therefore, c-di-AMP corresponds to an inverse agonist of A2a, since increasing its concentration affected the survival of monocytes even in the absence of A2a agonists, and increasing the A2a agonist concentration protected against the effects of c-di-AMP or cGAMP (Fig. 4D to G). These data demonstrate that extracellular c-di-AMP and cGAMP are inverse agonist ligands for A2a, whose tonic (agonist-free) signaling regulates the apoptosis of freshly isolated human monocytes. Importantly, ZM241385, another inverse agonist of A2a, was also slightly cytotoxic toward monocytes (Fig. 4A). Furthermore, in PBMCs transfected with A2a siRNA, a

FIG 2 Human monocytes selectively expressing the Adora2a gene and A2a adenosine receptor are c-di-AMP sensitive. (A) Freshly isolated PBMCs were cultured for 16 h in complete medium with increased doses of adenosine-based cyclic dinucleotides in the medium (extracellular) or using a transfection method (intracellular [red]). (B) Release of IFN-β from sorted human monocytes in culture with and without c-di-AMP (5 μM). (C) Monocytes were not depleted from PBMC cultures in complete medium supplemented with IFN-β. (D) Relative levels of STING mRNA expression and purinergic receptor-encoding genes (Affymetrix Human Genome U133 Plus 2.0 and Affymetrix Mouse Genome 430 2.0 microarrays) in the specified human and murine cell subsets. Means of values normalized to GAPDH are shown. (E) Specific binding of NECA-fluo to the specified human or murine cell subsets. Means shown are percent specific binding from nine independent measures of mean NECA-fluo signal intensity, with 0% binding obtained in cells without tracker and 100% binding obtained in cells with maximal fluorescence (e.g., [NECA-fluo] $>10^{-6}$ M). *, $P < 0.05$ (Student paired t test) versus controls. (F) Incubation of c-di-AMP with human or murine monocytes from PBMCs or splenocytes, respectively ($n = 4$ for murine cells and $n = 14$ for human cells). (G) Differential (CHO-A2a versus CHO) binding of solubilized purified cell membranes expressing A2a over immobilized c-di-AMP surface. (H) Differential (CHO-A2a versus CHO) binding of soluble c-di-AMP (100 μM) over surfaces coated with purified cell membranes expressing or not the A2a receptor.

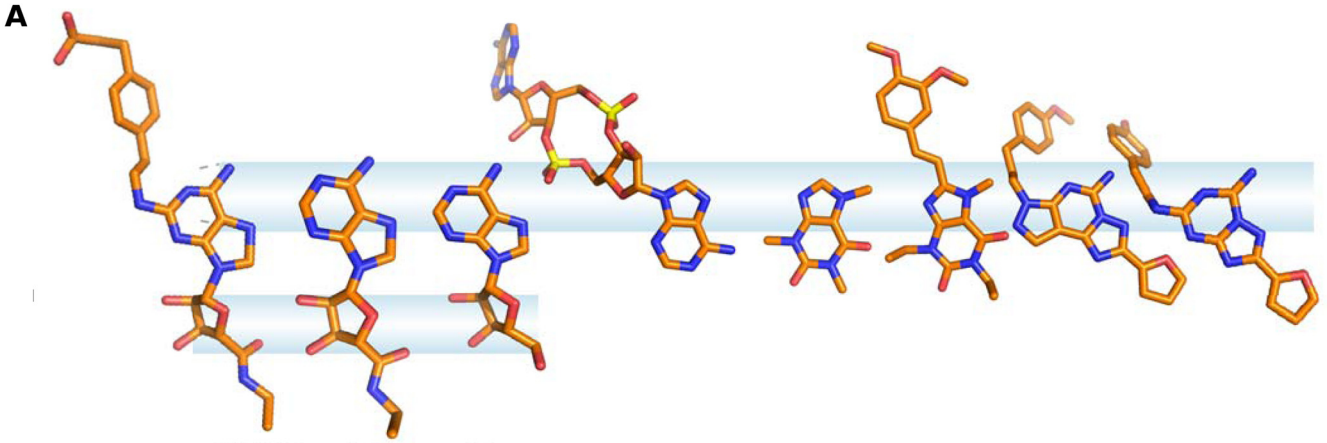

	CGS21680	NECA	Adenosine	c-di-AMP	Caffeine	Istradefylline	SCH442416	ZM241385
volume *	420	258	209	494	153	325	283	274
interaction N253	yes	yes	yes	yes	yes	yes	yes	yes
interaction H278	yes	yes	yes	no	no	no	no	no
interaction S277	yes	yes	yes	no	no	no	no	no
ΔG active $A_{2A}AR$ **	-9.5	-9.0	-8.0	-5.0	-5.5	>0	-3.6	-2.0
ΔG inactive $A_{2A}AR$ **	-8.4	-7.0	-6.0	-7.0	-6.5	-9.1	-8.3	-8.8
ligand type	agonist	agonist	agonist	-	antagonist	Inverse agonist	antagonist	Inverse agonist
EC_{50} or K_i ***	27	20	310	-	23400	12	4	2

* (Å); ** (kcal/mol); *** (nM)

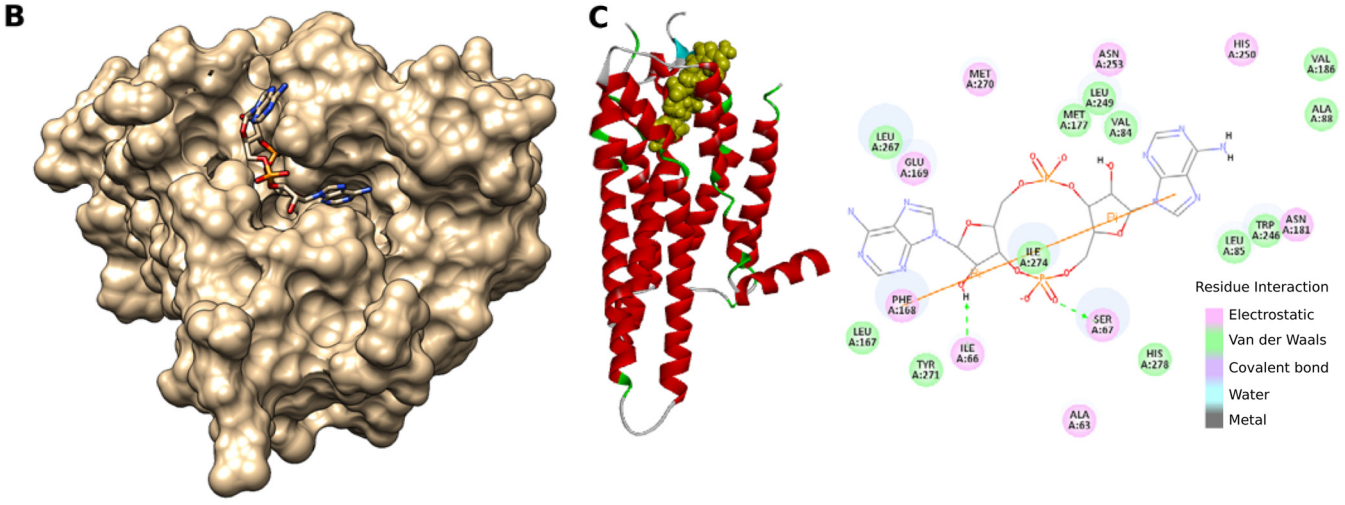

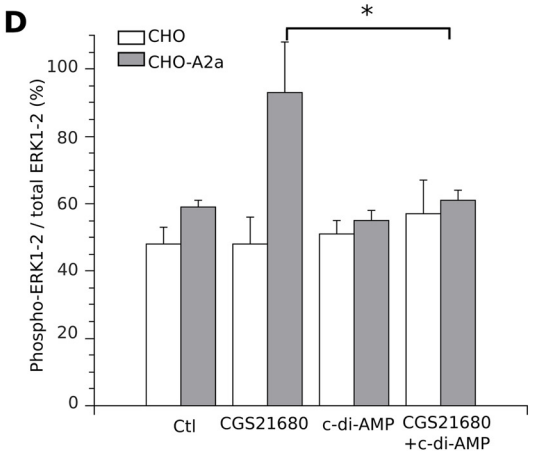

FIG 3 3′,5′ cyclic di-AMP is an antagonist/inverse agonist ligand of the human A2a adenosine receptor. (A) Structural comparison of c-di-AMP to known A2a ligands. The crystallized conformations of A2a-bound agonists, inverse agonists, and antagonists were aligned using their respective Asn253-binding atoms as a reference. The information summarizes the distinct A2a-binding patterns of agonists and antagonists and suggests that the A2a-binding conformation of

loss of $CD14^+$ monocytes was observed, even without the additional effects of c-di-AMP (Fig. 4H). Likewise, the pharmacological decoupling of A2a from its $G_{\alpha s}$ following treatment with suramin selectively depleted PBMCs of monocytes (Fig. 4A). Together, these data indicate that the loss of basal (agonist-free) A2a signaling was sufficient to kill the monocytes. This implies that if the loss of constitutive $G_{\alpha s}$ signaling is lethal for monocytes, its restoration by any means should rescue these cells. Accordingly, both the activation of other $G_{\alpha s}$-coupled monocyte GPCRs using prostaglandin E2 and the direct activation of adenylate cyclase using forskolin efficiently protected monocytes from c-di-AMP-induced apoptosis (Fig. 4C). Therefore, the lethality of the loss of A2a signaling in human monocytes can be complemented by other GPCR-driven pathways which provide these cells with tonic intracellular signaling.

Extinction of A2a tonic signaling induces mPTP-dependent apoptosis. The results shown in Fig. 2B and C indicate that STING activation and type I IFN responses did not account for the cytotoxicity of the extracellular cyclic dinucleotides. We therefore supposed that A2a signaling might be independent of this intracellular pathway. To check whether STING was engaged downstream of the A2a pathway, we used the THP1-Blue-hSEAP human monocyte cell line to monitor the activation of the human STING/IRF3 pathway. When their STING pathway is activated, THP1-Blue-hSEAP cells induce IRF3 and thus express a secreted embryonic alkaline phosphatase reporter gene. STING activation is then measured by the optical density (OD) of the chromogenic product of SEAP activity. cGAMP, c-di-AMP, and the other nucleotides activated STING at high (>10 μM) but not low extracellular concentrations (Fig. 5A), and none of the other A2a ligands caused STING activation (Fig. 5B). Furthermore, neither A2a signaling downstream of agonists nor that downstream of antagonists had any effect on a simultaneous STING response to cGAMP (Fig. 5C). Finally, inhibition of STING by dorsomorphin (23) did not reduce the toxicity of c-di-AMP (Fig. 5D). These results show that the A2a and STING pathways are independent of each other.

Next, we investigated the signaling pathways induced from the interaction of adenosine-based cyclic dinucleotides with A2a in monocytes. As with other inverse A2a agonists, c-di-AMP reduced the baseline level of intracellular cAMP and PKA activity in freshly isolated human monocytes without the addition of any exogenous adenosine to the media (Fig. 6A and B). Thus, c-di-AMP inhibited the tonic, constitutive signaling downstream of A2a in monocytes.

PKA activity, whose levels were lower in monocytes treated with c-di-AMP (Fig. 6A and B), is known to drive proteasomal degradation of cytosolic p53 (24, 25, 26). To further investigate c-di-AMP-induced signaling downstream of A2a, we looked at levels of p53. Stabilization of p53 promotes the opening of the mitochondrial permeability transition pore (mPTP), which can lead to apoptosis (27). We investigated the effect of extracellular c-di-AMP on p53 levels in human monocytes. Although c-di-AMP did not affect the total level of p53, it induced a striking accumulation of cytosolic p53 and decreased its nuclear fraction (Fig. 6C). Accordingly, the nucleus-localizing phospho-Ser315 p53 isoform was reduced in c-di-AMP-treated monocytes but not in lymphocytes from the same experiments (Fig. 6D). These observations suggested that c-di-AMP might induce the opening of the mPTP in monocytes. We therefore used flow cytometry to test formation of the mPTP at the single-cell level. This method showed that untreated monocytes were not apoptotic (annexin V^-), had functional mitochondria (Mitotracker green^{high}, Mitotracker deep red^{high}), and lacked the mPTP, as shown by their calcein fluorescence in the presence of $CoCl_2$ (mean fluorescence intensity [MFI], 9,911 [Fig. 6E]). In contrast, most c-di-AMP-treated monocytes had reduced viability and harbored dysfunctional mitochondria, with a lower calcein fluorescence (MFI, 8,187), reflecting mPTP opening. The persistence of calcein fluorescence in monocytes treated with a combination of c-di-AMP and cyclosporine (MFI, 9,415) confirmed this assumption, since the cyclophilin D-p53 complex forming the mPTP is inhibited by cyclosporine (28, 29) (Fig. 6E). Plotting the fluorescence of Mitotracker deep red against calcein showed that the loss of A2a signaling provoked the opening of mPTP (visualized as Mitotracker deep red^{low}, calcein^{low} cells in Fig. 6F). However, monocytes treated with A2a agonists or forskolin prevented c-di-AMP-induced opening of the mPTP (Fig. 6F).

Opening of the mPTP dissipates the mitochondrial proton gradient, yielding dysfunctional mitochondria. Therefore, c-di-AMP- and cGAMP-treated monocytes (but not T lymphocytes) and A2a siRNA-transfected monocytes harbor defective mitochondria (Fig. 4E and 6G and H). Cyclosporine protected against this defect, while p53 stabilization by the proteasome inhibitors lactacystine and MG132 accentuated it (Fig. 6I). In line with the kinetics of inhibition of PKA activity, c-di-AMP treatment reduced the respiration of monocytes, a defect arising from the loss of mitochondrial oxidative phosphorylation (Fig. 7A to C). This energetic deficit of monocytes was limited to their respiration, as their glycolysis was unaffected by c-di-AMP (Fig. 7B); however, it was sufficient to cause their apoptosis (Fig. 1G).

These results show that A2a signaling critically controls mitochondrial function in both monocytes (Fig. 6F to I and 7D) and CHO-A2a cells (Fig. 7C). As demonstrated using GPCR complementation assays, the c-di-AMP-induced mitochondrial defect can be prevented by A2a agonists or complemented by other cAMP-elevating drugs (Fig. 7D). In summary, the c-di-AMP inverse agonist blocks constitutive A2a signaling, inducing an accumulation of cytosolic p53 which opens the mPTP and impairs mitochondrial function, ultimately leading to monocyte apoptosis.

c-di-AMP induces apoptosis *in vivo* in human monocytes developing in NSG mice reconstituted with human cord blood $CD34^+$ cells. The results in Fig. 2E and F indicated that human but not murine monocytes are sensitive to cyclic dinucleotides; there-

c-di-AMP, predicted by molecular docking to bind to the inactive receptor (PDB code 3PWH), corresponds to an antagonist ligand. (B) Top-view model of c-di-AMP docked in the inactive A2a adenosine receptor (PDB code 3PWH). (C) Predicted interactions between c-di-AMP and A2a receptor. The corresponding tridimensional structure of the c-di-AMP/A2a complex is shown on the left, with inactive A2a conformation represented by red ribbons and c-di-AMP by spheres. The A2a residues interacting with c-di-AMP are indicated, color-coded by type of interaction. In this model, the A2a (N253) residue has electrostatic interaction with adenine, but neither A2a (S277) nor A2a (H278) interacts with the corresponding ribose 2′ OH. As illustrated in panel A, this pattern corresponds to A2a antagonists/inverse agonists. (D) Phosphorylation of ERK1/2 in CHO-A2a cells induced by A2a agonist CGS21680 (100 nM) is inhibited by c-di-AMP (10 μM). *, $P < 0.05$ (Student paired *t* test) for CHO-A2a cells treated with CGS21680 versus CHO-A2a cells treated with CGS21680 plus c-di-AMP.

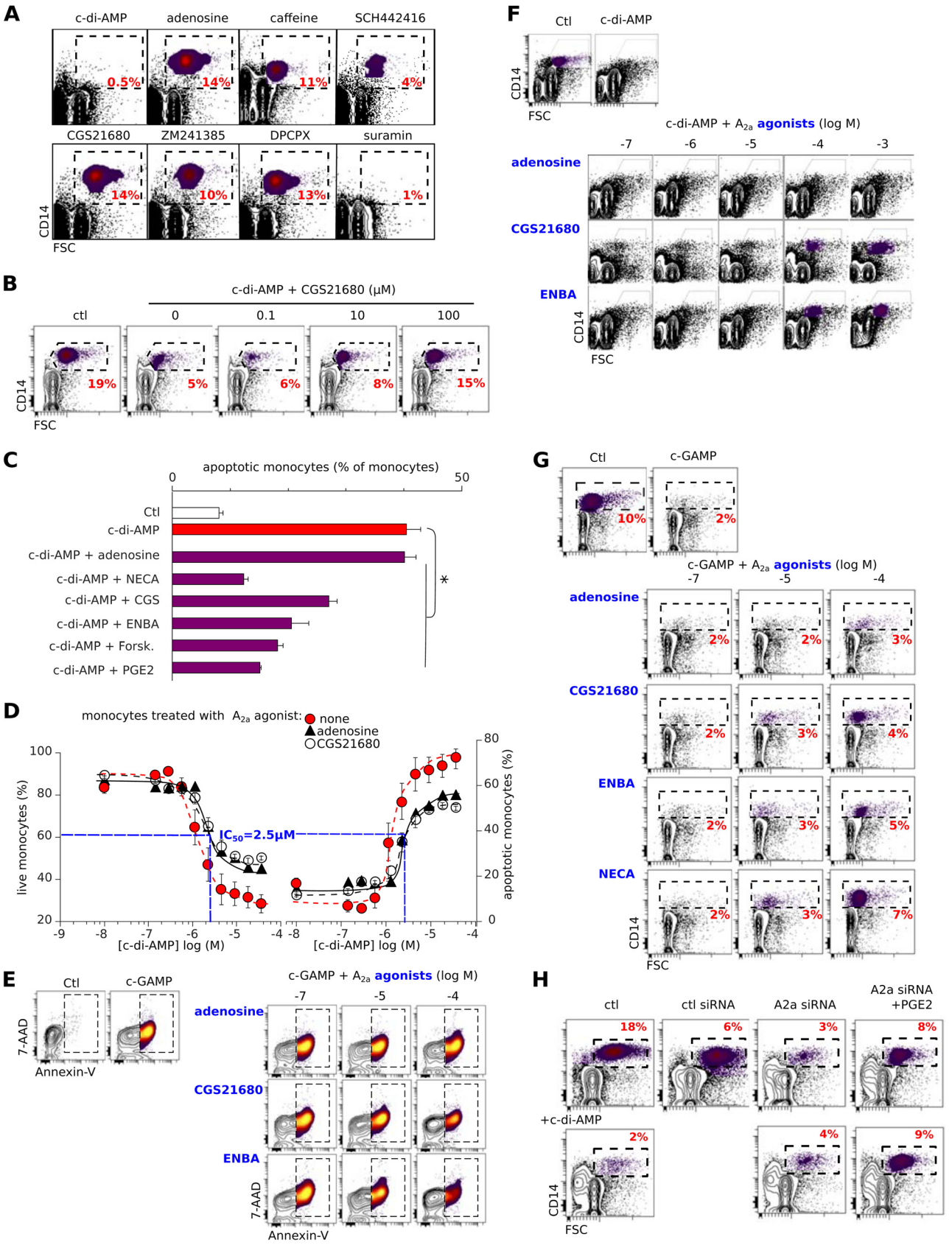
A
c-di-AMP
adenosine
caffeine
SCH442416
0.5%
14%
11%
4%
CGS21680
ZM241385
DPCPX
suramin
14%
10%
13%
1%
CD14
FSC
B
c-di-AMP + CGS21680 (μM)
ctl
0
0.1
10
100
19%
5%
6%
8%
15%
CD14
FSC
C
apoptotic monocytes (% of monocytes)
0
50
Ctl
c-di-AMP
c-di-AMP + adenosine
c-di-AMP + NECA
c-di-AMP + CGS
c-di-AMP + ENBA
c-di-AMP + Forsk.
c-di-AMP + PGE2
*
D
monocytes treated with A2a agonist:
none
adenosine
CGS21680
live monocytes (%)
apoptotic monocytes (%)
IC50=2.5μM
[c-di-AMP] log (M)
[c-di-AMP] log (M)
E
Ctl
c-GAMP
7-AAD
Annexin-V
c-GAMP + A2a agonists (log M)
-7
-5
-4
adenosine
CGS21680
ENBA
7-AAD
Annexin-V
F
Ctl
c-di-AMP
CD14
FSC
c-di-AMP + A2a agonists (log M)
-7
-6
-5
-4
-3
adenosine
CGS21680
ENBA
CD14
FSC
G
Ctl
c-GAMP
10%
2%
c-GAMP + A2a agonists (log M)
-7
-5
-4
adenosine
2%
2%
3%
CGS21680
2%
3%
4%
ENBA
2%
3%
5%
NECA
2%
3%
7%
CD14
FSC
H
ctl
ctl siRNA
A2a siRNA
A2a siRNA +PGE2
18%
6%
3%
8%
+c-di-AMP
2%
4%
9%
CD14
FSC

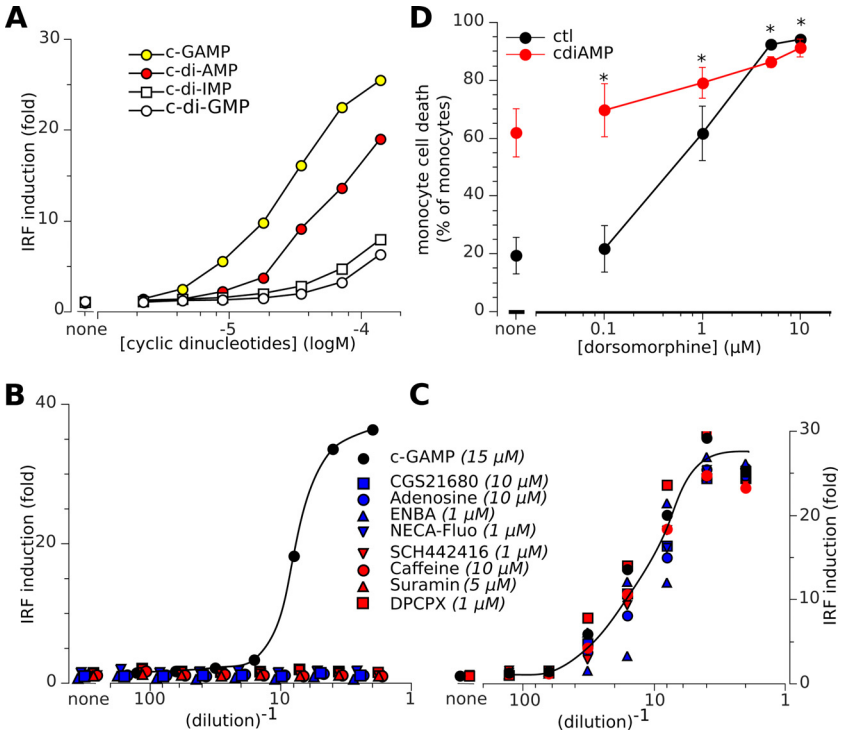

FIG 5 Independence of the human A2a and STING pathways. (A to C) The THP1-Blue-hSEAP human monocyte line was used for monitoring of the human STING/IRF3 pathway. When their STING pathway is activated, THP1-Blue-hSEAP cells induce IRF3 and thus express a secreted embryonic alkaline phosphatase reporter gene under the control of an ISG54 promoter in conjunction with five IFN-stimulated response elements. Hence, STING activation is measured by the OD (655 nm) of the chromogenic product of SEAP activity and expressed as fold change normalized to baseline levels in resting cells. (A) When THP1-Blue-hSEAP cells are exposed to various extracellular cyclic dinucleotides, their human STING pathway is activated. In contrast to the A2a pathway (Fig. 1D), c-di-AMP is less potent than cGAMP for activation of the human STING/IRF3 pathway. (B) Alone, agonist and antagonist ligands of the A2a receptor, or suramin (stock concentrations specified in italics), do not activate the STING pathway downstream from the A2a pathway. (C) Modulation of the A2a receptor pathway by A2a agonists and antagonists or by suramin does not affect simultaneous activation of the STING pathway by cGAMP (15 μM). (D) Monocytes are treated with increased doses of dorsomorphin with (red) and without (black) c-di-AMP (5 μM). Data are means ± SD from more than five independent experiments. *, $P < 0.05$ (paired Student *t* test).

fore, to assess the physiological relevance of the proapoptotic activity of c-di-AMP *in vivo*, we used a human immune system (HIS) mouse model. This had the advantage of allowing us to evaluate the effect of c-di-AMP on all hematopoietic lineages. We monitored human hematopoietic cell engraftment in NOD/SCID/$\gamma_c^{-/-}$ (NSG) mice after intrahepatic injection of human cord blood $CD34^+$ cells prestimulated with cytokines (TPO, 20 ng/ml; SCF, 100 ng/ml; and Flt-3L, 100 ng/ml) (30, 31, 32). Mice treated with c-di-AMP and control mice showed the same levels of human $CD34^+$ progenitor cells in the bone marrow (Fig. 8A). In contrast, c-di-AMP-treated mice showed a strong decrease in splenic $CD13^+$ myelomonocytic precursor cells relative to the amount in control animals (Fig. 8B). Importantly, these mice also showed a clear-cut reduction of $CD14^+$ monocytes in the spleen, blood, and, to a lesser extent, bone marrow (Fig. 8C). This decrease was due to the apoptosis of monocytes (Fig. 8D). As no cell loss or apoptotic cells were detected in human lymphoid subsets from the same animals (Fig. 8E and F), this apoptosis was specific to monocytes. Of note, human $CD13^+$ myeloid precursors expressed levels of A2a receptors similar to those expressed by monocytes, while

FIG 4 Ligands of A2a regulate monocyte apoptosis induced by c-di-AMP and cGAMP. (A) c-di-AMP (5 μM) but not the A2a agonists adenosine and CGS21680 (100 μM) deplete monocytes. The A2a antagonists/inverse agonists caffeine, SCH244416, and ZM241385 (100 μM) or the A2a decoupler suramin (100 μM) also depletes monocytes, but less efficiently. The percentages of monocytes are indicated in the dashed boxes. (B and C) Monocytes were rescued from c-di-AMP-induced cell death in the same assay as for panel A, either by the A2a agonist CGS21680 (B) or by other c-AMP-raising drugs (100 μM) (C). Data are means ± SD from more than five independent experiments. *, $P < 0.05$ (paired Student *t* test) versus monocytes treated with c-di-AMP. (D) Monocyte death or survival as a measurement of the competition for A2a by agonists and c-di-AMP. Shown are the percentages of live (left) or apoptotic (annexin V^+) (right) monocytes among PBMCs that had been incubated for 16 h in complete medium with either of the A2a agonists adenosine (310 nM) and CGS21680 (30 nM) and the indicated concentrations of c-di-AMP. Means and SD from six independent experiments are shown. (E) Monocyte (FSC^{high} $CD14^+$ cells, boxed) death/survival after 24 h of *in vitro* PBMC culture with c-GAMP (5 μM) and the specified concentrations of A2a agonists. Representative results from six independent experiments are shown. (F and G) Monocytes (FSC^{high} $CD14^+$ cells, boxed) after 16 h of *in vitro* PBMC culture with c-di-AMP (F) or cGAMP (G) (5 μM) and the specified concentrations of A2a agonists. The monocyte depletion by c-di-AMP or cGAMP was avoided by the highest concentrations of CGS21680 and ENBA agonists, while 1 mM adenosine weakly protected the monocytes. Representative results from six independent experiments are shown. (H) Freshly isolated PBMCs were transfected with control or A2a siRNA with or without c-di-AMP (5 μM) and stained for CD14. Representative results from three independent experiments are shown.

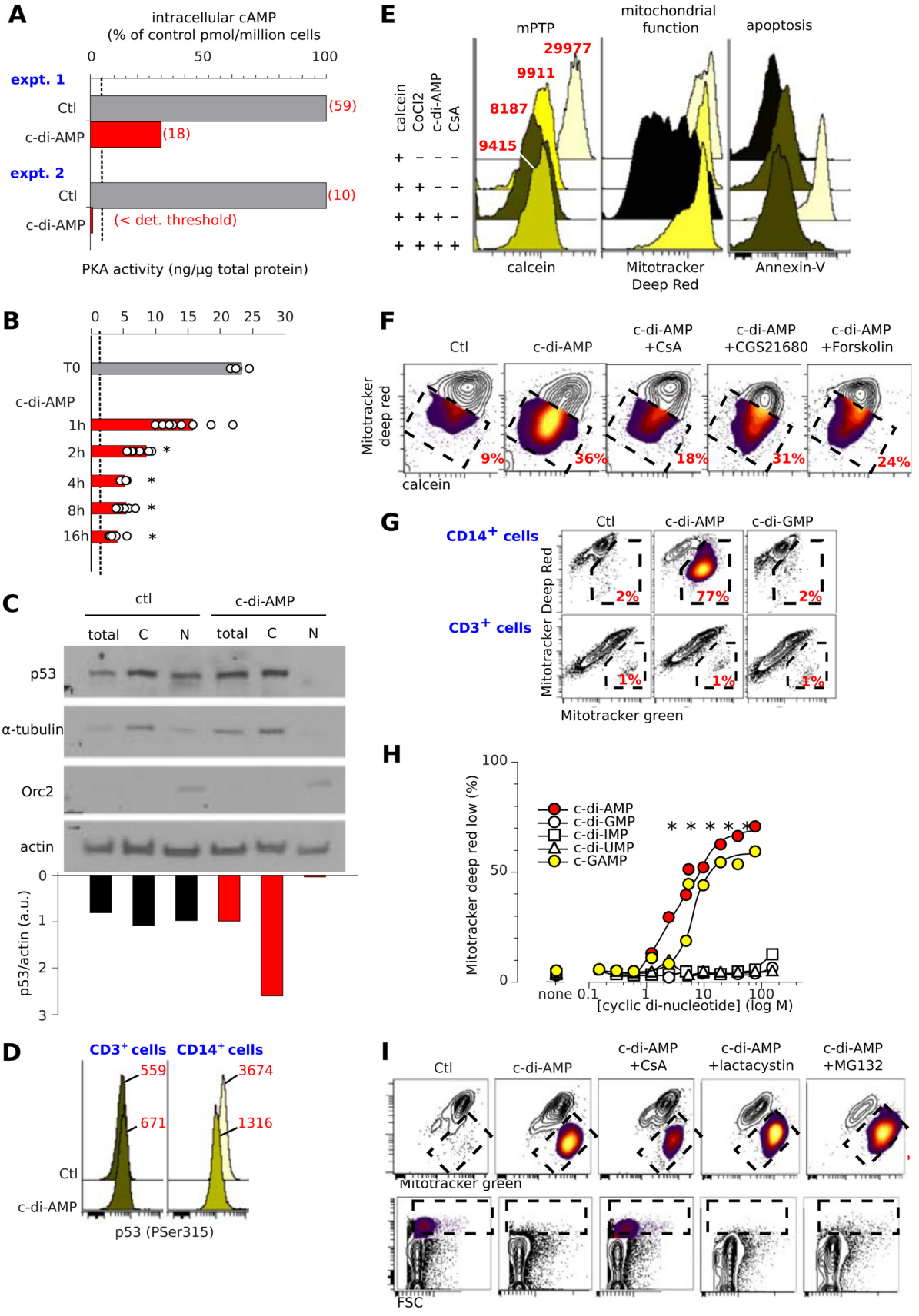
A
intracellular cAMP
(% of control pmol/million cells
0
50
100
expt. 1
Ctl
(59)
c-di-AMP
(18)
expt. 2
Ctl
(10)
c-di-AMP
(< det. threshold)
PKA activity (ng/µg total protein)
B
0
5
10
15
20
25
30
T0
c-di-AMP
1h
2h
4h
8h
16h
C
ctl
c-di-AMP
total
C
N
total
C
N
p53
α-tubulin
Orc2
actin
p53/actin (a.u.)
0
1
2
3
D
CD3+ cells
CD14+ cells
559
671
3674
1316
Ctl
c-di-AMP
p53 (PSer315)
E
mPTP
mitochondrial function
apoptosis
29977
9911
8187
9415
calcein
CoCl2
c-di-AMP
CsA
calcein
Mitotracker Deep Red
Annexin-V
F
Ctl
c-di-AMP
c-di-AMP +CsA
c-di-AMP +CGS21680
c-di-AMP +Forskolin
Mitotracker deep red
9%
36%
18%
31%
24%
calcein
G
CD14+ cells
CD3+ cells
Ctl
c-di-AMP
c-di-GMP
2%
77%
2%
1%
1%
1%
Mitotracker Deep Red
Mitotracker green
H
100
50
0
Mitotracker deep red low (%)
c-di-AMP
c-di-GMP
c-di-IMP
c-di-UMP
c-GAMP
none
0.1
1
10
100
[cyclic di-nucleotide] (log M)
I
Ctl
c-di-AMP
c-di-AMP +CsA
c-di-AMP +lactacystin
c-di-AMP +MG132
Mitotracker green
FSC

$CD34^+$ common progenitors, granulocyte/macrophage progenitors, megakaryocyte/erythrocyte precursors, promyelocytes (Fig. 8G), and all mature lymphocytes (Fig. 2D) did not express it. Thus, these data demonstrate that c-di-AMP selectively affects human monocytes and their $CD13^+$ myelocyte precursors *in vivo* through an A2a-mediated mechanism.

DISCUSSION

This study demonstrated that extracellular cyclic dinucleotides containing adenosine constitute inverse agonists of the A2a adenosine receptor, abrogating its downstream signaling. In freshly isolated human $CD14^+$ monocytes expressing A2a, this abrogation allows the accumulation of cytosolic p53, which mediates the formation of the mPTP and mitochondrial dysfunction leading to apoptosis. *In vivo*, c-di-AMP induces a clear-cut decrease in splenic human $CD13^+$ myelocytes, which also express the A2a gene Adora2a. In contrast, the monomyelocytic cell line THP1 coexpresses the adenosine receptor A2a alongside A2b and A3, which differ in their $G_{\alpha s}$ coupling, and harbors a partial deletion of the p53 gene (33). No mPTP or apoptotic response to c-di-AMP was seen in this cell line. Although many different human tissues and cell types express one or more of the four adenosine receptors, the apoptotic response to these cyclic dinucleotides was observed only in normal myeloid cells with a selective expression of A2a. Importantly, no such response was detected in any human $CD34^+$ progenitor cell subsets or $CD45^+$ lymphoid cell lineages in HIS NSG mice, leading to a deficit exclusively delineated to monocytes and $CD13^+$ myelomonocytic precursor in the human hematopoietic cell population. This provides a new method for depleting monocytes from human PBMCs or other hematopoietic tissues, an objective which was previously achieved using clodronate-laden liposomes (34). These data also suggest that mammalian cells expressing A2a receptors can detect extracellular c-di-AMP or cGAMP, as illustrated in this study by their selective recognition by human monocytes. Although the cell surface A2a receptor and mPTP induction pathway differ from the intracellular STING-type I IFN pathway (4, 5) (Fig. 5), the sensing of these extracellular cyclic dinucleotides leads to cell death. Hence, when released from damaged or infected human tissues, these compounds represent monocyte-targeting toxins. Clearly, their potential impact on host-pathogen interactions during infections deserves further investigation.

The cell surface expression of A2a in mammalian brain, heart, kidney, liver, vasculature, and hematopoietic tissues allows a variety of homeostatic functions (reviewed in reference 17), including cell survival in response to adenosine (35, 36). It is possible that cyclic dinucleotides affect these homeostatic functions. Nevertheless, until now, a blockade of A2a signaling has never been described as a direct trigger of apoptosis. Our report establishes this link for the first time. *In vivo* pharmacological studies of Adora2a knockout mice and animal models have demonstrated that A2a ligands are neuroprotective, but the mechanism is unclear, as both A2a antagonists (37, 38) and agonists (39, 40) were neuroprotective. A2a antagonism/inverse agonism is clearly a promising target in the treatment of human Parkinson's disease (41), as both caffeine intake (42) and genetic polymorphisms of the Adora2a gene (43) contribute to the risk of contracting the disease. Furthermore, in the study of Parkinson's disease, promising results have been obtained with istradefylline, an inverse agonist specific to A2a (44). Thus, cyclic dinucleotides constitute a potential novel class of A2a inverse agonist, with pharmacokinetics, pharmacodynamics, and safety profiles distinctive from those of istradefylline.

The capacity to induce cell survival or apoptosis according to the ligand posits A2a as a dependence receptor (45). The A2a-mediated proapoptotic pathway nevertheless diverges from the classical cell-extrinsic apoptosis pathway that dependence receptors use for negative signal transduction (46). The regulatory A2a-mPTP axis depicted here merges cell-extrinsic and cell-intrinsic apoptosis. It also unveils GPCR-mediated control of the transcription-independent but proteasome-sensitive activity of p53. This pathway is reminiscent of but different from both A2a agonist-induced transcriptional upregulation of Bid (47) and p53-mediated transcriptional upregulation of the adenosine receptor A2b, which promotes Bcl-2/Puma-dependent apoptosis (48). However, the apoptotic resistance to adenylate cyclase blockade by A2b agonists (48) probably results from the induction of the mPTP. Thus, A2a- and A2b-driven apoptotic pathways might involve common steps. How cells coexpressing A2a and A2b respond to

FIG 6 The A2a inverse agonist c-di-AMP induces mPTP-dependent cell death. (A to D) Extracellular c-di-AMP affects intracellular cAMP, PKA, and p53. Treatment of purified human monocytes (10^7 cells per assay) with c-di-AMP (5 μM) reduces cytosolic cAMP (italics: pmol/million monocytes) (A) and inhibits PKA activity (ng of activity per μg of total cytosolic protein) (B). Bars show means from eight independent experiments; dots show individual data. *, $P < 0.05$ (paired Student *t* test) versus untreated cells. (C) c-di-AMP induces p53 relocalization. (Top) Western blots of p53 from c-di-AMP-treated and control monocytes in whole-cell (total), nuclear (N), and cytosolic (C) extracts. The purity of these fractions was checked by labeling for Orc2 (nuclear fraction) and α-tubulin (cytoplasm). (Bottom) p53 densitometric quantification relative to actin. (D) Flow cytometry of cells labeled for intracellular phospho-Ser315 of p53 shows a reduction in nuclear p53 in c-di-AMP-treated monocytes (MFIs are in red), while staining with isotype control was unaffected under the same conditions (MFI = 95 [data not shown]). (E) Flow cytometry assay for the mPTP. Shown are histograms of calcein, Mitotracker deep red, and annexin V fluorescence of gated monocytes tested in the specified settings. CsA, cyclosporine. MFIs are indicated in red. Representative results from more than three independent experiments are shown. Cells were loaded with the cell-permeant calcein AM (upper track). Upon addition of the calcein fluorescence quencher $CoCl_2$, the fluorescence of cytoplasmic calcein is lost, while that of mitochondria is retained. Upon c-di-AMP treatment, however, opening of the mPTP allows quenching of mitochondrial calcein fluorescence, but CsA protects this quenching by inhibiting the mPTP. (F) c-di-AMP induces opening of the mPTP. Contour plots of flow cytometry mPTP assays in monocytes gated from PBMCs treated as specified with c-di AMP (5 μM), CsA (100 μM), CGS21680 (100 μM), or forskolin (100 μM) are shown. Decreased calcein fluorescence indicates the mPTP, and a decreased Mitotracker deep red signal indicates dysfunctional mitochondria; dashed boxes show cells with the mPTP and the percentages. Representative results from four independent experiments are shown. (G) Representative results of contour plots showing that c-di-AMP but not c-di-GMP induces mitochondrial dysfunction (Mitotracker deep red fluorescence) but not total mitochondria (Mitotracker green fluorescence) from monocytes but not lymphocytes in the same experiments. Dashed boxes show cells with mitochondrial dysfunction and their percentages. (H) Titration of the cyclic dinucleotide bioactivity on reduction of the mitochondrial function in monocytes. Shown are means from eight independent experiments. *, $P < 0.05$ (paired Student *t* test) versus control. (I) c-di-AMP-induced mPTP opening reduces mitochondrial function (Mitotracker deep red fluorescence) but not total mitochondria (Mitotracker green fluorescence) (top row) and depletes monocytes from PBMCs (bottom row). Cells were treated with CsA (100 μM), lactacystin (10 μM), and MG132 (10 μM) as specified.

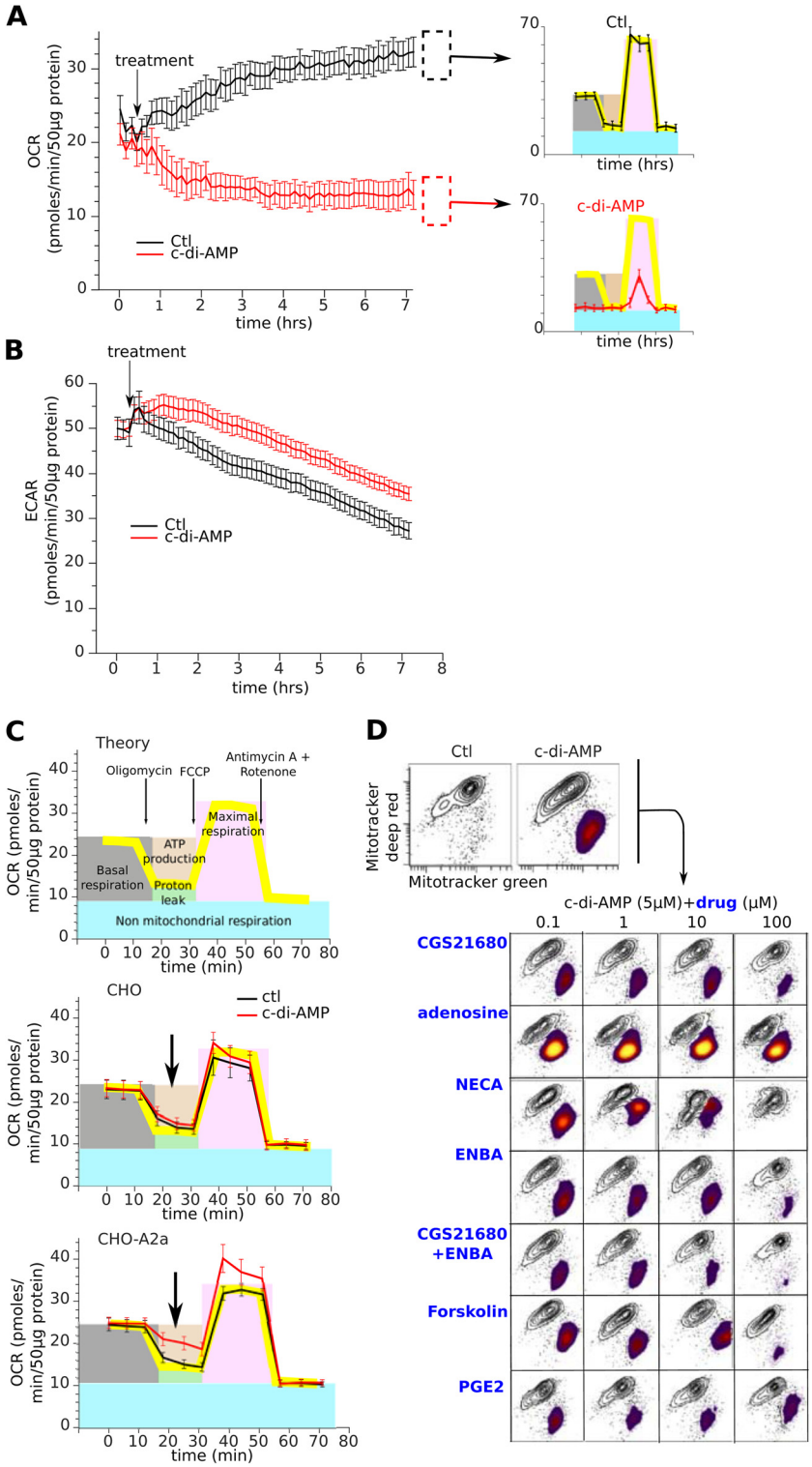

FIG 7 c-di-AMP induces formation of the mPTP and defective mitochondrial function. (A and B) The bioenergetic profiles of purified human monocytes treated with c-di-AMP (5 M) were determined using the extracellular flux analyzer. The rates of oxygen consumption (OCR, an indicator of mitochondrial respiration) (A) and extracellular acidification (ECAR, an indicator of glycolysis) (B) were followed for 6 h after treatment. OCR was followed by sequential injection of oligomycin (1 μM), carbonyl cyanide-4-(trifluoromethoxy)phenylhydrazone (FCCP) (1 μM), and antimycin A plus rotenone (1 μM) to determine the indices of mitochondrial function (top right). Data are means ± SD from representative donor profiles; six assay replicates were carried out per sample. (C) Same as for panel A but using CHO or CHO-A2a cells. Data are means ± SD from representative assay profiles; six assay replicates were carried out per sample. (D) Mitochondrial dysfunction induced by A2a antagonism can be rescued by A2a agonists or other cAMP-elevating drugs.

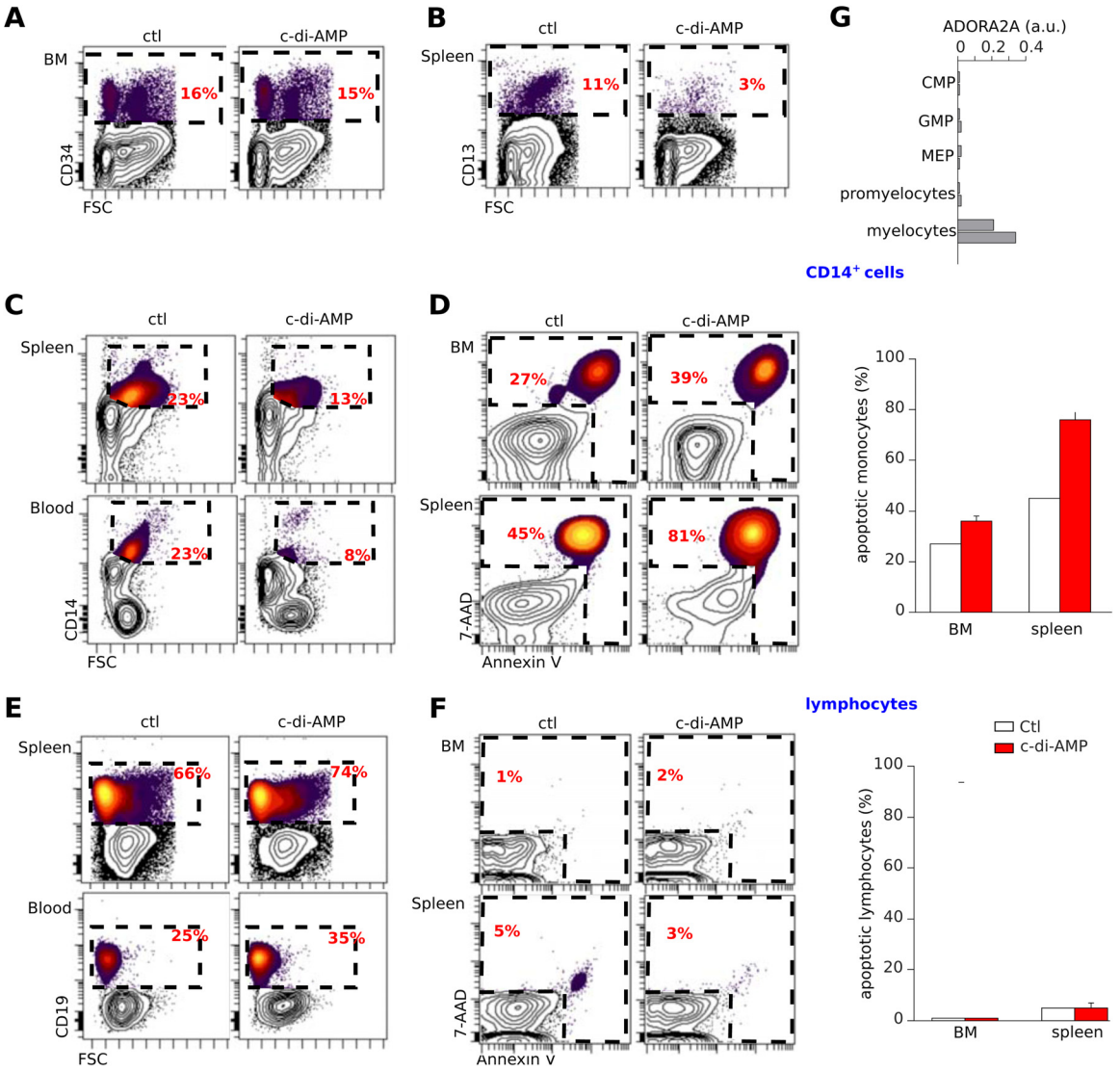

FIG 8 c-di-AMP induces apoptosis of human monocytes and myeloid precursors developing in NSG mice reconstituted with human CD34$^+$ cells. (A to G) Newborn NSG mice engrafted with human cord blood CD34$^+$ cells showing >30% human CD45$^+$ cells in the blood after 10 weeks of reconstitution were injected with 2 cycles of c-di-AMP (50 μg) or PBS (100 μl). Forty-eight hours after injection, the hematopoietic tissues of these mice were stained and compared. (A) Bone marrow (BM) CD34$^+$ progenitor cells were not affected by c-di-AMP, whereas the numbers of CD13$^+$ myelocytes and splenocytes were reduced in these mice (B). The number of human CD14$^+$ monocytes was reduced in blood, spleen, and marrow of c-di-AMP-treated mice (C) as they were undergoing apoptosis (D). (E and F) Human B cell development was unaffected by c-di-AMP. Representative rates and apoptotic phenotypes of B cells from the same animals as shown in panels C and D are shown. The right images show composites of results (mean and SEM; $n = 7$). (G) Relative levels of mRNA expression of *Adora2a* gene (Affymetrix Human Genome U133 Plus 2.0 microarray) in human common myeloid precursor (CMP) CD34$^+$ cells, granulocyte/macrophage progenitor (GMP) CD34$^+$ cells, megakaryocyte/erythrocyte progenitor (MEP) CD34$^+$ cells, promyelocytes, and CD13$^+$ myelocytes. Data were extracted from the GEO data set under accession number GSE19599 (10) and normalized to GAPDH as for Fig. 2D.

agonists and antagonist ligands, and the wiring of their respective signal transduction pathways, remains to be determined. The implications of cytosolic p53 controlling steady-state GPCR signaling extend the physiological significance of the nontranscriptional functions of p53 beyond the surveillance of oxidative stress or ischemia. When facing oxidative stress, p53 orchestrates a necrotic response (49), whereas detection of degraded A2a tonic signaling by cytosolic p53 induces apoptosis. Such discrimination allows p53 to connect the type of stress with the immunogenicity of the dying cells, which differs for apoptotic and necrotic cells.

Finally, this report opens new therapeutic perspectives for mPTP-driven pathologies, since GPCRs are highly druggable targets. The A2a inverse agonist activity of adenosine-based cyclic dinucleotides introduces new drug candidates for pathologies such as A2a-related neurodegeneration (50, 51) or A2b-sensitive triple-negative breast carcinomas (52). As representatives of a structurally new class of GPCR ligands, cyclic dinucleotides could also inspire the design of new drugs. Although most A2a antagonists are currently derived from xanthine structures (17), cyclic dimers of the reference agonist, adenosine, turn out to be antagonists/inverse agonists. Whether new antagonists/inverse agonists

of other GPCRs can be likewise rationally designed, i.e., as cyclic dimers of their respective agonist ligand, is an exciting possibility that now needs to be examined.

ACKNOWLEDGMENTS

We acknowledge the technical advice from members of the laboratory of J.-J.F. and Isabelle Loubinoux (INSERM U825, Toulouse, France) and Guillaume Lebon (IGF Montpellier) for Adora2a cDNA and CHO cells. We are grateful to Nancy Aubry for critical reading and Kelly Thornber for editing of the manuscript.

This study was funded by INSERM, Université de Toulouse III Paul Sabatier, CNRS, and by contracts from INCa (TUMOSTRESS), Institut Carnot Lymphome (CALYM), and Laboratoire d 'Excellence Toulouse Cancer (TOUCAN).

REFERENCES

1. **Pesavento C, Hengge R.** 2009. Bacterial nucleotide-based second messengers. Curr Opin Microbiol **12:**170–176. http://dx.doi.org/10.1016/j.mib.2009.01.007.
2. **Chen Z-H, Schaap P.** 2012. The prokaryote messenger c-di-GMP triggers stalk cell differentiation in Dictyostelium. Nature **488:**680–683. http://dx.doi.org/10.1038/nature11313.
3. **Gao D, Wu J, Wu Y-T, Du F, Aroh C, Yan N, Sun L, Chen ZJ.** 2013. Cyclic GMP-AMP synthase is an innate immune sensor of HIV and other retroviruses. Science **341:**903–906. http://dx.doi.org/10.1126/science.1240933.
4. **Wu J, Sun L, Chen X, Du F, Shi H, Chen C, Chen ZJ.** 2013. Cyclic GMP-AMP is an endogenous second messenger in innate immune signaling by cytosolic DNA. Science **339:**826–830. http://dx.doi.org/10.1126/science.1229963.
5. **Sun L, Wu J, Du F, Chen X, Chen ZJ.** 2013. Cyclic GMP-AMP synthase is a cytosolic DNA sensor that activates the type I interferon pathway. Science **339:**786–791. http://dx.doi.org/10.1126/science.1232458.
6. **Zhou R, Yazdi AS, Menu P, Tschopp J.** 2011. A role for mitochondria in NLRP3 inflammasome activation. Nature **469:**221–225. http://dx.doi.org/10.1038/nature09663.
7. **Pont F, Familiades J, Dejean S, Fruchon S, Cendron D, Poupot M, Poupot R, L'faqihi-Olive F, Prade N, Ycart B, Fournie J-J.** 2012. The gene expression profile of phosphoantigen-specific human T lymphocytes is a blend of T-cell and NK-cell signatures. Eur J Immunol **42:**228–240. http://dx.doi.org/10.1002/eji.201141870.
8. **Compagno M, Lim WK, Grunn A, Nandula SV, Brahmachary M, Shen Q, Bertoni F, Ponzoni M, Scandurra M, Califano A, Bhagat G, Chadburn A, Dalla-Favera R, Pasqualucci L.** 2009. Mutations of multiple genes cause deregulation of NF-kappaB in diffuse large B-cell lymphoma. Nature **459:**717–721. http://dx.doi.org/10.1038/nature07968.
9. **Miyara M, Yoshioka Y, Kitoh A, Shima T, Wing K, Niwa A, Parizot C, Taflin C, Heike T, Valeyre D, Mathian A, Nakahata T, Yamaguchi T, Nomura T, Ono M, Amoura Z, Gorochov G, Sakaguchi S.** 2009. Functional delineation and differentiation dynamics of human CD4+ T cells expressing the FoxP3 transcription factor. Immunity **30:**899–911. http://dx.doi.org/10.1016/j.immuni.2009.03.019.
10. **Andersson A, Pedén Olofsson T, Fioretos T.** 2010. Gene expression signatures in childhood acute leukemias are largely unique and distinct from those of normal tissues and other malignancies. BMC Med Genomics **3:**6. http://dx.doi.org/10.1186/1755-8794-3-6.
11. **Bennett KA, Tehan B, Lebon G, Tate CG, Weir M, Marshall FH, Langmead CJ.** 2013. Pharmacology and structure of isolated conformations of the adenosine A2A receptor define ligand efficacy. Mol Pharmacol **83:**949–958. http://dx.doi.org/10.1124/mol.112.084509.
12. **Lebon G, Tate CG.** 2011. Structure of the adenosine-bound conformation of the human adenosine A(2A) receptor. Med Sci (Paris) **27:**926–928. http://dx.doi.org/10.1051/medsci/20112711004.
13. **Grosdidier A, Zoete V, Michielin O.** 2011. SwissDock, a protein-small molecule docking web service based on EADock DSS. Nucleic Acids Res **39:**W270–W277. http://dx.doi.org/10.1093/nar/gkr366.
14. **Van Damme T, Zhang Y, Lynen F, Sandra P.** 2012. Determination of cyclic guanosine-and cyclic adenosine monophosphate (cGMP and cAMP) in human plasma and animal tissues by solid phase extraction on silica and liquid chromatography—triple quadrupole mass spectrometry. J Chromatogr B Analyt Technol Biomed Life Sci **909:**14–21. http://dx.doi.org/10.1016/j.jchromb.2012.10.002.
15. **Petronilli V, Miotto G, Canton M, Brini M, Colonna R, Bernardi P, Lisa FD.** 1999. Transient and long-lasting openings of the mitochondrial permeability transition pore can be monitored directly in intact cells by changes in mitochondrial calcein fluorescence. Biophys J **76:**725–734. http://dx.doi.org/10.1016/S0006-3495(99)77239-5.
16. **Witte CE, Whiteley AT, Burke TP, Sauer J-D, Portnoy DA, Woodward JJ.** 2013. Cyclic di-AMP is critical for Listeria monocytogenes growth, cell wall homeostasis, and establishment of infection. mBio **4**(3):e00282–13. http://dx.doi.org/10.1128/mBio.00282-13.
17. **Jacobson KA, Gao Z-G.** 2006. Adenosine receptors as therapeutic targets. Nat Rev Drug Discov **5:**247–264. http://dx.doi.org/10.1038/nrd1983.
18. **Brand F, Klutz AM, Jacobson KA, Fredholm BB, Schulte G.** 2008. Adenosine A2a receptor dynamics studied with the novel fluorescent agonist Alexa488-APEC. Eur J Pharmacol **590:**36–42. http://dx.doi.org/10.1016/j.ejphar.2008.05.036.
19. **Lebon G, Warne T, Edwards PC, Bennett K, Langmead CJ, Leslie AGW, Tate CG.** 2011. Agonist-bound adenosine A2A receptor structures reveal common features of GPCR activation. Nature **474:**521–525. http://dx.doi.org/10.1038/nature10136.
20. **Venkatakrishnan AJ, Deupi X, Lebon G, Tate CG, Schertler GF, Babu MM.** 2013. Molecular signatures of G-protein-coupled receptors. Nature **494:**185–194. http://dx.doi.org/10.1038/nature11896.
21. **Schulte G, Fredholm BB.** 2000. Human adenosine A1, A2A, A2B, and A3 receptors expressed in Chinese hamster ovary cells all mediate the phosphorylation of extracellular-regulated kinase 1/2. Mol Pharmacol **58:**477–482.
22. **Inoue A, Ishiguro J, Kitamura H, Arima N, Okutani M, Shuto A, Higashiyama S, Ohwada T, Arai H, Makide K, Aoki J.** 2012. TGF alpha shedding assay: an accurate and versatile method for detecting GPCR activation. Nat Methods **9:**1021–1029. http://dx.doi.org/10.1038/nmeth.2172.
23. **Konno H, Konno K, Barber GN.** 2013. Cyclic dinucleotides trigger ULK1 (ATG1) phosphorylation of STING to prevent sustained innate immune signaling. Cell **155:**688–698. http://dx.doi.org/10.1016/j.cell.2013.09.049.
24. **Zhang F, Hu Y, Huang P, Toleman CA, Paterson AJ, Kudlow JE.** 2007. Proteasome function is regulated by cyclic AMP-dependent protein kinase through phosphorylation of Rpt6. J Biol Chem **282:**22460–22471. http://dx.doi.org/10.1074/jbc.M702439200.
25. **Safa M, Kazemi A, Zand H, Azarkeivan A, Zaker F, Hayat P.** 2010. Inhibitory role of cAMP on doxorubicin-induced apoptosis in pre-B ALL cells through dephosphorylation of p53 serine residues. Apoptosis **15:**196–203. http://dx.doi.org/10.1007/s10495-009-0417-8.
26. **Safa M, Kazemi A, Zaker F, Razmkhah F.** 2011. Cyclic AMP-induced p53 destabilization is independent of EPAC in pre-B acute lymphoblastic leukemia cells in vitro. J Recept Signal Transduct Res **31:**256–263. http://dx.doi.org/10.3109/10799893.2011.578140.
27. **Pediaditakis P, Kim J-S, He L, Zhang X, Graves LM, Lemasters JJ.** 2010. Inhibition of the mitochondrial permeability transition by protein kinase A in rat liver mitochondria and hepatocytes. Biochem J **431:**411–421. http://dx.doi.org/10.1042/BJ20091741.
28. **Crompton M, Ellinger H, Costi A.** 1988. Inhibition by cyclosporin A of a Ca2+-dependent pore in heart mitochondria activated by inorganic phosphate and oxidative stress. Biochem J **255:**357–360.
29. **Broekemeier K, Dempsey M, Pfeiffer D.** 1989. Cyclosporin A is a potent inhibitor of the inner membrane permeability transition in liver mitochondria. J Biol Chem **264:**7826–7830.
30. **Ito M, Kobayashi K, Nakahata T.** 2008. NOD/Shi-scid IL2rnull (NOG) mice more appropriate for humanized mouse models. Curr Top Microbiol Immunol **324:**53–76. http://dx.doi.org/10.1007/978-3-540-75647-7_3.
31. **Shima H, Takubo K, Iwasaki H, Yoshihara H, Gomei Y, Hosokawa K, Arai F, Takahashi T, Suda T.** 2009. Reconstitution activity of hypoxic cultured human cord blood CD34-positive cells in NOG mice. Biochem Biophys Res Commun **378:**467–472. http://dx.doi.org/10.1016/j.bbrc.2008.11.056.
32. **Cai S, Wang H, Bailey B, Hartwell JR, Silver JM, Juliar BE, Sinn AL, Baluyut AR, Pollok KE.** 2011. Differential secondary reconstitution of in vivo-selected human SCID-repopulating cells in NOD/SCID versus NOD/SCID/g chain null mice. Bone Marrow Res **2011:**252953. http://dx.doi.org/10.1155/2011/252953.
33. **Sugimoto K, Toyoshima H, Sakai R, Miyagawa K, Hagiwara K,**

Ishikawa F, Takaku F, Yazaki Y, Hirai H. 1992. Frequent mutations in the p53 gene in human myeloid leukemia cell lines. Blood **79:**2378–2383.
34. **Schmidt-Weber C, Rittig M, Buchner E, Hauser I, Schmidt I, Palombo-Kinne E, Emmrich F, Kinne RW.** 1996. Apoptotic cell death in activated monocytes following incorporation of clodronate-liposomes. J Leukoc Biol **60:**230–244.
35. **Crossman D, Whyte M.** 1993. Adenosine-A2 receptor stimulation of human neutrophils inhibits programmed cell-death (apoptosis). Circulation **88:**545–545.
36. **Boucher M, Wann B, Kaloustian S, Cardinal R, Godbout R, Rousseau G.** 2006. Reduction of apoptosis in the amygdala by an A2A adenosine receptor agonist following myocardial infarction. Apoptosis **11:**1067–1074. http://dx.doi.org/10.1007/s10495-006-6313-6.
37. **Kalda A, Yu L, Oztas E, Chen J-F.** 2006. Novel neuroprotection by caffeine and adenosine A2A receptor antagonists in animal models of Parkinson's disease. J Neurol Sci **248:**9–15. http://dx.doi.org/10.1016/j.jns.2006.05.003.
38. **Yu L, Shen H-Y, Coelho J E, Arajo IM, Huang Q-Y, Day Y-J, Rebola N, Canas PM, Rapp EK, Ferrara J, Taylor D, Mller CE, Linden J, Cunha RA, Chen J-F.** 2008. Adenosine A2A receptor antagonists exert motor and neuroprotective effects by distinct cellular mechanisms. Ann Neurol **63:**338–346. http://dx.doi.org/10.1002/ana.21313.
39. **Mayne M, Fotheringham J, Yan H-J, Power C, Del Bigio MR, Peeling J, Geiger JD.** 2001. Adenosine A2A receptor activation reduces proinflammatory events and decreases cell death following intracerebral hemorrhage. Ann Neurol **49:**727–735. http://dx.doi.org/10.1002/ana.1010.
40. **Cassada DC, Tribble CG, Long SM, Kaza AK, Linden J, Rieger JM, Rosin D, Kron IL, Kern JA.** 2002. Adenosine A2A agonist reduces paralysis after spinal cord ischemia: correlation with A2A receptor expression on motor neurons. Ann Thorac Surg **74:**846–850. http://dx.doi.org/10.1016/S0003-4975(02)03793-1.
41. **Chen J-F, Xu K, Petzer JP, Staal R, Xu Y-H, Beilstein M, Sonsalla PK, Castagnoli K, Castagnoli N, Jr, Schwarzschild MA.** 2001. Neuroprotection by caffeine and A (2A) adenosine receptor inactivation in a model of Parkinsons disease. J Neurosci **21:**RC143.
42. **Ross GW, Abbott RD, Petrovitch H, Morens DM, Grandinetti A, Tung K-H, Tanner CM, Masaki KH, Blanchette PL, Curb JD, Popper JS, White LR.** 2000. Association of coffee and caffeine intake with the risk of Parkinson disease. JAMA **283:**2674–2679. http://dx.doi.org/10.1001/jama.283.20.2674.
43. **Lin J, Yueh K.** 2013. Genetic polymorphism of adenosine A2a receptor is associated with the development of Parkinson's disease and of L-dopa-induced hyperkinesia. Mov Disord **28:**S39.
44. **Chen W, Wang H, Wei H, Gu S, Wei H.** 2013. Istradefylline, an adenosine A2A receptor antagonist, for patients with Parkinson's disease: a meta-analysis. J Neurol Sci **324:**21–28. http://dx.doi.org/10.1016/j.jns.2012.08.030.
45. **Mehlen P, Bredesen DE.** 2000. Dependence receptors: links between apoptosis, nervous system development and control of tumorigenesis. Bull Cancer **87:**537–541. (In French.)
46. **Mehlen P.** 2005. The dependence receptor notion: another way to see death. Cell Death Differ **12:**1003. http://dx.doi.org/10.1038/sj.cdd.4401708.
47. **Tamura K, Kanno T, Fujita Y, Gotoh A, Nakano T, Nishizaki T.** 2012. A2a adenosine receptor mediates HepG2 cell apoptosis by downregulating Bcl-XL expression and upregulating bid expression. J Cell Biochem **113:**1766–1775. http://dx.doi.org/10.1002/jcb.24048.
48. **Long JS, Crighton D, O'Prey J Mackay G, Zheng L, Palmer TM, Gottlieb E, Ryan KM.** 2013. Extracellular adenosine sensing—a metabolic cell death priming mechanism downstream of p53. Mol Cell **50:**394–406. http://dx.doi.org/10.1016/j.molcel.2013.03.016.
49. **Vaseva AV, Marchenko ND, Ji K, Tsirka SE, Holzmann S, Moll UM.** 2012. p53 opens the mitochondrial permeability transition pore to trigger necrosis. Cell **149:**1536–1548. http://dx.doi.org/10.1016/j.cell.2012.05.014.
50. **Hauser RA, Cantillon M, Pourcher E, Micheli F, Mok V, Onofrj M, Huyck S, Wolski K.** 2011. Preladenant in patients with Parkinson's disease and motor fluctuations: a phase 2, double-blind, randomised trial. Lancet Neurol **10:**221–229. http://dx.doi.org/10.1016/S1474-4422(11)70012-6.
51. **Schapira AHV, Bezard E, Brotchie J, Calon F, Collingridge GL, Ferger B, Hengerer B, Hirsch E, Jenner P, Novre NL, Obeso J A, Schwarzschild MA, Spampinato U, Davidai G.** 2006. Novel pharmacological targets for the treatment of Parkinson's disease. Nat Rev Drug Discov **5:**845–854. http://dx.doi.org/10.1038/nrd2087.
52. **Desmet CJ, Gallenne T, Prieur A, Reyal F, Visser NL, Wittner BS, Smit MA, Geiger TR, Laoukili J, Iskit S, Rodenko B, Zwart W, Evers B, Horlings H, Ajouaou A, Zevenhoven J, van Vliet M, Ramaswamy S, Wessels LFA, Peeper DS.** 2013. Identification of a pharmacologically tractable Fra-1/ADORA2B axis promoting breast cancer metastasis. Proc Natl Acad Sci U S A **110:**5139–5144. http://dx.doi.org/10.1073/pnas.1222085110.